

**PETRU PONI
INSTITUTE OF
MACROMOLECULAR
CHEMISTRY**



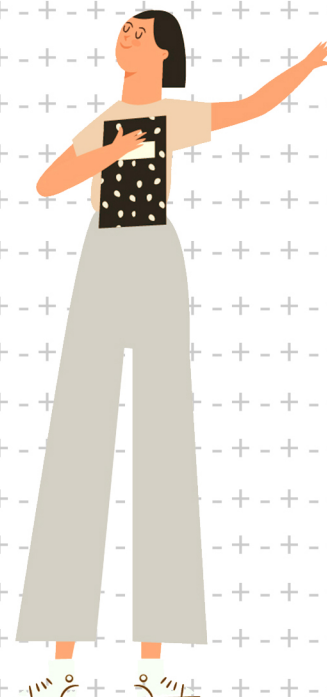
ICMPP

**OPEN
DOOR
TO THE
FUTURE**

**SCIENTIFIC
COMMUNICATIONS
OF YOUNG
RESEARCHERS**

2nd Edition

**November 19, 2021
Iasi, Romania**



Marking the Romanian Researcher's Day



ICMPP – OPEN DOOR TO THE FUTURE
SCIENTIFIC COMMUNICATIONS OF
YOUNG RESEARCHERS

2nd Edition

November 19, 2021 • Iasi • Romania

Marking the Romanian Researcher's Day

Organizer



Petru Poni Institute of Macromolecular Chemistry – ICMPP



The scientific communications event is organized by “Petru Poni” Institute of Macromolecular Chemistry - ICMPP, to mark the Romanian Researcher’s Day and offers the opportunity to young researchers (doctoral and postdoctoral students) to present the results of their studies.



The scientific program includes oral presentations (15 minutes, Q & A included) and the conference language will be English.



CONTACT

Email: macroyouth@icmpp.ro

Website: <https://icmpp.ro/events/conferences/macroyouth.php>



SCIENTIFIC BOARD

Chair: Dr. Valeria HARABAGIU
Acad. Bogdan C. SIMIONESCU

Members: Dr. Mariana PINTEALA
Dr. Sergiu COSERI
Dr. Luminita MARIN
Dr. Marcela MIHAI
Dr. Gheorghe FUNDUEANU
Dr. Maria CAZACU
Dr. Mariana-Dana DAMACEANU
Dr. Anton AIRINEI
Dr. Mariana CRISTEA



ORGANIZING BOARD

Chair: Dr. Petrisor SAMOILA
Members: Dr. Marcela MIHAI
Dr. Florin BUCATARIU
Dr. Corneliu COJOCARU
Secretary: Dr. Andra-Cristina HUMELNICU
Support IT: Catalin Buzdugan



SCIENTIFIC PROGRAM

MACROYOUTH OPENING		
9.00-9.05	https://us06web.zoom.us/j/84906488032 Dr. Valeria Harabagiu, ICMPP Director	
9.05-9.50	Dielectric elastomer transducers INVITED LECTURE Dorina M. Opris <i>Swiss Federal Laboratories for Materials Science and Technology Empa, Laboratory for Functional Polymers, Dübendorf, Switzerland</i>	Page 5
SESSION 1 – Oral Communications		
09.50-11.20	https://us06web.zoom.us/j/84906488032 Chair: Dr. Petrisor Samoila	
09.50-10.05	Development of bioactive hydrogels containing <i>Thymus Vulgaris</i> essential oil by ice template-assisted freeze-drying technique <u>Ioana-Victoria Platon</u> , Irina Elena Raschip, Ana Clara Aprotosoiaie, Adina Catinca Gradinaru, Maria Valentina Dinu	Page 7
10.05-10.20	Synthesis and characterization of novel imine derivatives of quaternary ammonium salt of chitosan <u>Bianca-Iustina Andreica</u> , Irina Rosca, Luminita Marin	Page 9
10.20-10.35	Improved domain and selectivity for uric acid detection using as sensitive materials complexes between an amino functionalized porphyrin and CuNPs, PtNPs or Pt@CuNPs Camelia Epuran	Page 11
10.35-10.50	Biodegradable imino-chitosan nanofibers as wound dressing materials <u>Alexandru Anisiej</u> , Irina Rosca, Andreea-Isabela Sandu, Adrian Bele, Luminita Marin	Page 13
10.50-11.05	Novel luminescent phenothiazine derivatives for biological applications <u>Sandu Cibotaru</u> , Luminita Marin	Page 15
11.05-11.20	Xanthan as component of the drug delivery systems <u>Alexandra Dimofte</u> , Narcis Anghel, Maria Valentina Dinu, Iuliana Spiridon	Page 17
11.20-11.35	Cofee break	

SESSION 2 – Oral Communications

11.35-12.50

<https://us06web.zoom.us/j/84906488032>

Chair: Dr. Corneliu Cojocaru

11.35-11.50	ROBOSAMPLE: robotics-based Gibbs sampling of macro-molecular systems	Page 19
-------------	---	---------

Teodor Asvadur Șulea, Eliza Cristina Martin, Victor Gabriel Ungureanu, Laurențiu Spiridon, Andrei-Jose Petrescu

11.50-12.05	Ionic beads/CaCO₃ composites as sorbents for small organic molecules	Page 21
-------------	--	---------

Ana-Lavinia Vasiliu, Marius-Mihai Zaharia, Marcela Mihai

12.05-12.20	Efficient recovery of wastewaters based on beneficial interferences between porphyrin derivatives, platinum nanoparticles and silica mesoporous matrices	Page 23
-------------	---	---------

Ion Fratilescu

12.20-12.35	Composite materials based on polyelectrolytes - sorbents in batch and column studies	Page 25
-------------	---	---------

Larisa-Maria Petrilă, Florin Bucatariu, Marcela Mihai

12.35-12.50	Composite membranes based on sulfonated poly(ether ether ketone) with potential application in fuel cell	Page 27
-------------	---	---------

Laurențiu Baltag, Petrisor Samoila, Adriana T. Marinoiu, Corneliu Cojocaru, Valeria Harabagiu

12.50-14.00	Lunch break	
-------------	-------------	--

SESSION 3 – Oral Communications

14.00-15.15

<https://us06web.zoom.us/j/84906488032>

Chair: Dr. Florin Bucatariu

14.00-14.15	Mono- and oligonuclear complexes based on schiff base ligand	Page 29
-------------	---	---------

Ildiko Buta, Sergiu Shova, Sorina Ilies, Florica Manea, Marius Andruh, Otilia Costisor

14.15-14.30	Elucidation of complex structures through mass spectrometry fragmentation studies	Page 31
-------------	--	---------

Diana-Andreea Blaj, Mihaela Balan-Porcarasu, Valeria Harabagiu, Cristian Peptu

14.30-14.45	Synthesis and characterization of novel polyurethanes based on piperazine and renewable cross-linkers	Page 33
-------------	--	---------

Violeta Otilia Potolinca, Stefan Oprea

14.45-15.00	Multi-step procedure leading to a heterocycle containing dimethylsilane unit	Page 35
-------------	---	---------

Madalin Damoc, Alexandru Constantin Stoica, Diana Blaj, Ana-Maria Macsim, Mihaela Dascalu, Maria Cazacu

15.00-15.15	Triapine analogues and their copper(II) complexes: synthesis, characterization, solution behavior, redox activity, cytotoxicity and mR2 RNR inhibition	Page 37
	<u>Iuliana Besleaga</u> , Iryna Stepanenko, Tatsiana V. Petrasheuskaya, Denisa Darvasiova, Martin Breza, Marta Hammerstad, Małgorzata A. Marć, Alexander Roller, Gabriella Spengler, Ana Popović-Bijelić, Eva A. Enyedy, Peter Rapta, Anatoly D. Shutalev, Vladimir B. Arion	
15.15-15.30	Cofee break	
SESSION 4 – Oral Communications		
15.30-17.00	https://us06web.zoom.us/j/84906488032 Chair: Dr. Marcela Mihai	
15.30-15.45	Enhanced photodegradation of Evans Blue by novel samarium doped zinc aluminium spinel ferrites	Page 39
	<u>Greucu Ionela</u> , Samoilă Petrișor, Corneliu Cojocaru, Petronela Pascariu, Valeria Harabagiu	
15.45-16.00	Xanthan acrylate/cobalt ferrite material for removing dyes from wastewaters	Page 41
	<u>Irina Apostol</u> , Narcis Anghel, Iuliana Spiridon	
16.00-16.15	<i>In silico</i> studies of a novel amphiphilic graft conjugated polymer for biomedical applications	Page 43
	<u>Petru Țirnovan</u> , Francesca Mocci, Tudor Vasiliu, Luminița Cianga, Ioan Cianga, Mariana Pinteală, Aatto Laaksonen	
16.15-16.30	Zwitterionic porous microparticles -Advanced materials as potential drug delivery systems	Page 45
	<u>Marin-Aurel Trofin</u> , Stefania Racovita, Silvia Vasiliu, Ana-Lavinia Vasiliu, Marcela Mihai	
16.30-16.45	pH/temperature-sensitive interpenetrating polymeric hydrogel	Page 47
	<u>Bogdan Cosman</u> , Sanda Bucatariu, Marieta Constantin, G. Fundueanu	
16.45-17.00	Copper tetranuclear complex bearing silanol functional groups	Page 49
	<u>Alexandru-Constantin Stoica</u> , Madalin Damoc, Mihaela Dascalu, Maria Cazacu	
17.00-17.05	MACROYOUTH CLOSING	



BOOK OF ABSTRACTS

DIELECTRIC ELASTOMER TRANSDUCERS

Dorina M. Opris,^{1*} Yauhen Sheima,^{1,2} Simon Dünki,^{1,2} Elena Perju,^{1,3} Mihaela Alexandu,^{1,3} ohannes von Szczepanski,^{1,4} Patrick Danner,^{1,4} Mihail Iacob,¹ Song Ko,^{1,2} Francis Owusu,^{1,2} Jose Quinsaat,^{1,2} Frank Nüesch^{1,2}

¹Swiss Federal Laboratories for Materials Science and Technology Empa, Laboratory for Functional Polymers, Dübendorf, Switzerland.

²Ecole Polytechnique Federale de Lausanne, Lausanne, Switzerland

³Petru Poni Institute of Macromolecular Chemistry of Romanian Academy, Iasi, Romania

⁴Department of Materials, ETH Zurich, Zurich, Switzerland

*dorina.opris@empa.ch

Transducers are electrical components that convert one form of energy into another. Simplest transducers consist of two electrodes that sandwich a dielectric in between. However, such devices are rigid and not compliant. Contrary, dielectric elastomer transducers are elastic, compliant, and respond to an external stimulus when adequately designed.^[1]

This presentation will overview how we achieve stretchable electrodes and smart dielectric elastomers that respond to, sense, generate, or store electricity.

Stretchable electrodes can be synthesized by making composites of conductive fillers in an elastic matrix. As a conductive filler, we use graphene, and as a matrix, a silicone elastomer. Most reported conductive elastomers require the use of solvent, either for the synthesis of matrix or composites or for processing into thin films. In contrast, our composite is solvent-free, which enables printing on virtually any substrate without detrimental interferences observed otherwise.

Stimuli responsiveness in our transducers is introduced through polar amorphous polymers with randomly dispersed dipoles (Figure 1).^[2]

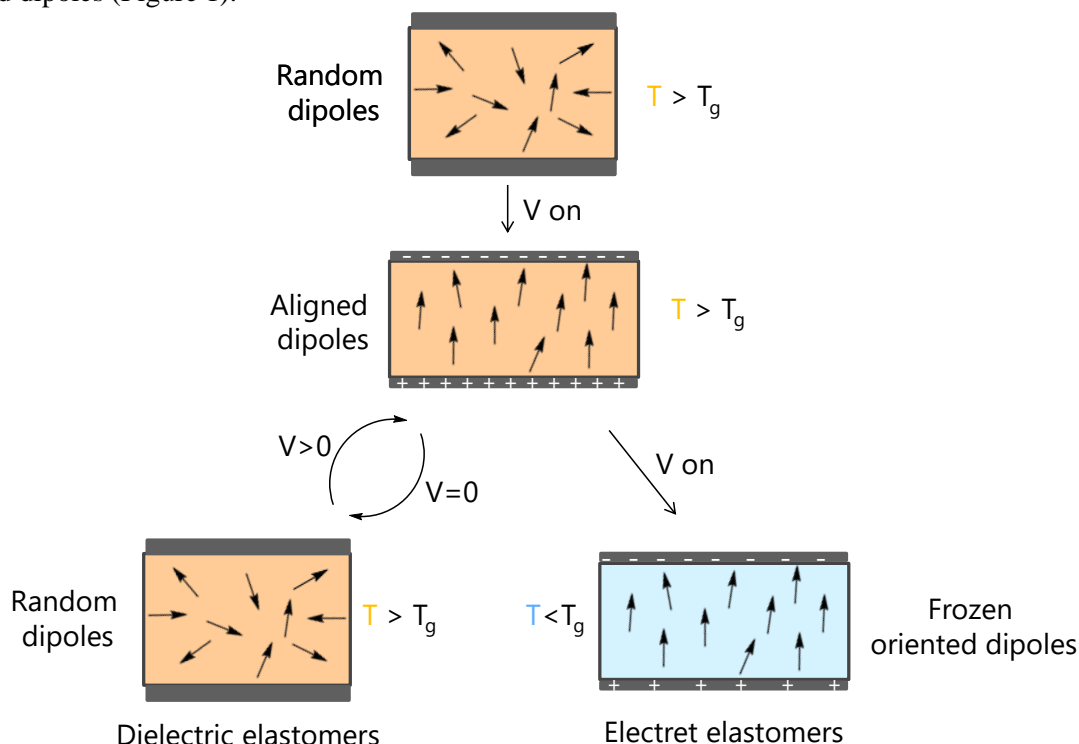


Figure 1. The use of polar groups to introduce functionality in polymers

Below the glass transition temperature (T_g), the polymer is a glassy solid and has an elastic modulus in the GPa range. Below T_g , if the capacitor is charged, the dielectric will not deform. If the polymer is heated above T_g , several important changes occur in the material: the elastic modulus changes several orders of magnitude and the dipoles are mobile. If the polymer is exposed to an electric field, it will deform, and if properly cross-linked, the polymer comes back to the original shape after the electric field is removed. If the polymer is cooled below T_g in an electric field, the oriented dipoles can be frozen and a permanent polarization can be introduced in the material.^[3]

Polar amorphous elastomers above T_g can be used as dielectrics in actuators, generators, and sensors. Such elastomers respond to a lower electric field, generate more energy per cycle, and have higher sensitivity in sensors as compared to conventional elastomers. Additionally, polar elastomers are also attractive as solid electrolytes for Li-ion batteries.^[4] The polar groups allow dissolving a significant amount of lithium salts needed for enhanced ionic conductivity, the low T_g facilitate Li-ion mobility during battery operation, while the elastic network allows hysteresis-free operation since it can accommodate significant volumetric changes during charging-discharging.

This presentation will also give an overview of how the synthesized polar polymers are manufactured into useful actuators, sensors, generators, and energy storage devices.^{[5][6][7]}

References

- [1] N. America, B. C. Burchfiel, P. W. Lipman, T. Parsons, G. Soc, A. Bull, A. Tovish, G. Schubert, B. P. Luyendyk, R. Pelrine, R. Kornbluh, Q. Pei, J. Joseph, *Science*, 2000, 287, 836.
- [2] D. M. Opris, *Adv. Mater.* **2018**, 30, 1703678.
- [3] Y. S. Ko, F. A. Nüesch, D. Damjanovic, D. M. Opris, *Adv. Mater.* 2017, 29, 1.
- [4] C. Fu, M. Iacob, Y. Sheima, C. Battaglia, L. Duchêne, L. Seidl, D. M. Opris, A. Remhof, *J. Mater. Chem. A* 2021, 9, 11794.
- [5] Y. Sheima, P. Caspari, D. M. Opris, *Macromol. Rapid Commun.* 2019, 40, 1.
- [6] Y. Sheima, Y. Yuts, H. Frauenrath, D. M. Opris, *Macromolecules* 2021, 54, 5737.
- [7] Y. J. Lee, P. Caspari, D. M. Opris, F. A. Nüesch, S. Ham, J. H. Kim, S. R. Kim, B. K. Ju, W. K. Choi, *J. Mater. Chem. C* 2019, 7, 3535.

Acknowledgment:

We gratefully acknowledge the Swiss National Science Foundation (IZERZO_142215, 200020_172693, 206021_150638/1, IZSAZ2_173358/1), the European Research Council (ERC) under the European Union's Horizon 2020 research and innovation programme (grant agreement No. 101001182), and the Swiss Federal Laboratories for Materials Science and Technology (Empa, Dübendorf) for financial support.

DEVELOPMENT OF BIOACTIVE HYDROGELS CONTAINING *THYMUS VULGARIS* ESSENTIAL OIL BY ICE TEMPLATE-ASSISTED FREEZE-DRYING TECHNIQUE

**Ioana-Victoria Platon^{1*}, Irina Elena Raschip¹, Ana Clara Aprotosoae²,
Adina Catinca Gradinaru², Maria Valentina Dinu¹**

¹*Petru Poni Institute of Macromolecular Chemistry, Department of Functional Polymers, Iasi, Romania*

²*“Grigore T. Popa” University of Medicine and Pharmacy, Iasi, Romania*

*platon.victoria@gmail.com

Thymus sp. is a series of plants belonging to the family *Lamiaceae* that are used both in traditional and modern medicine for a considerable number of therapeutical properties of which the most important are the antimicrobial, the antioxidant, the expectorant and the digestive ones [1]. Their well-recognised biological potential is mostly due to the presence of the essential oil, and that is why they are also called “aromatic species”. Although essential oils (EOs) have a wide range of medicinal properties, the preparation of highly efficient formulations is difficult because of their high volatility, high susceptibility to oxidative degradation during storage and under exposure to light, heat, air and moisture [2,3]. In regard to this, the embedding of EOs into polymer matrices based on natural macromolecules [4] is a promising approach to: (i) prevent the oxidation and volatilization, (ii) enhance the stability and water solubility, (iii) prolong the shelf-life, (iv) increase the bioavailability and efficacy, and (v) enable the controlled release of EOs.

In this context, we entrap here the EOs extracted from *Thymus vulgaris* (Thy) into a physically cross-linked biocompatible matrix based on chitosan/dextrins (CS/Dex) blends [5]. In addition, to obtain CS/Dex cryogel films with a sponge-like morphology, we selected the ice template-assisted freeze-drying technique (**Figure 1**). This freeze-thawing approach is a facile and eco-friendly method to prepare porous materials as the ice crystals act as pore-forming agents. Moreover, the 3D structure is mainly stabilized through the multiple intermolecular hydrogen bonds formed in the junction points of the polysaccharide network, which allowed us to avoid the use of toxic cross-linkers or harsh chemical treatments, and to prevent the formation of undesired by products.

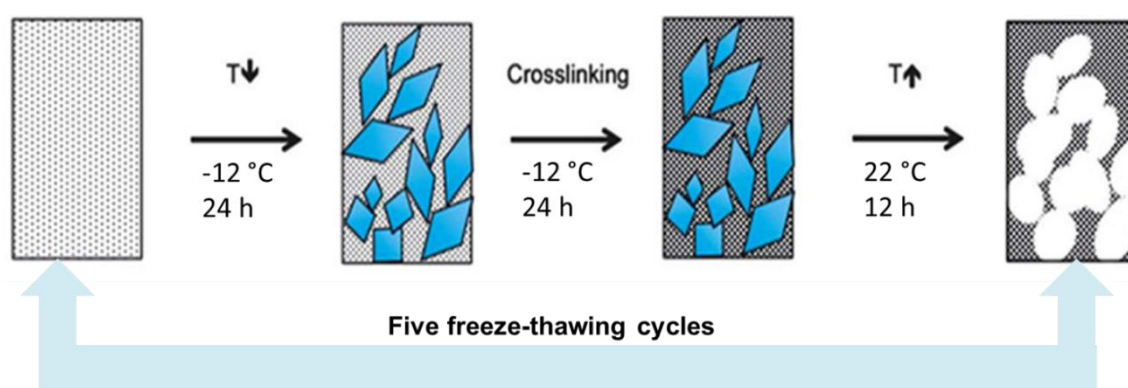


Figure 1. Preparations of the films

The Thy EO-loaded CS/Dex sponge films were characterized by Fourier transform infrared (FTIR) spectroscopy, scanning electron microscopy (SEM), moisture content, water solubility, swelling degree, and uniaxial compression measurements as a function of both Thy-loaded amount and CS molar mass. To establish the potential therapeutic functionality of these films, their antioxidant and antifungal activities were also evaluated [5]. The chemical profile of Thy EO showed thymol, a phenolic compound known for its strong antioxidant activity, as the main component (55.40 %). The content of embedded oil had a significant effect

on pore size and compressive properties of cryogel films. The swollen Thy-containing cryogel films showed fast shape recovery after full compression and water addition. The enhancement of mechanical performance and the lower swelling ratios of Thy-containing cryogel films indicate hydrogen bonding as the main interaction between cryogel components. The entrapment of thyme EO confers good *in vitro* antioxidant (Table 1) and anti-Candida activities [5]. These properties could be useful in skin candidiasis or onychomycosis treatment.

Table 1. Antioxidant activity of CS/Dex films containing Thy EO

Sample	DPPH radical scavenging activity (%)		ABTS ^{•+} radical scavenging activity (%)	
	5 min	2 h	5 min	2h
CS/Dex	-	-	-	
CS ₁₈₉ EO _{0.2%}	15.33±0.12	45.49±0.25	24.50±0.18	65.01±0.14
CS ₁₈₉ EO _{2%}	25.73±0.24	62.97±0.31	21.09±0.21	63.44±0.35
CS ₃₃₀ EO _{2%}	24.00±0.15	29.33±0.14	17.82±0.22	53.84±0.24
EO	21.12±0.15%	49.37±0.23	56.23±0.15	58.12±0.25

References

- [1] Z.-J. Ni, X. Wang, Y. Shen, et al., *Trends Food Sci. Technol.* 2021, 110, 78–89.
- [2] S. Tiwari, B.K. Singh, N.K. Dubey. *J. Sci. Res.* 2020, 64, 175-178.
- [3] C. Turek, F.C. Stintzing, *Compr. Rev. Food Sci. Food Saf.* 2013, 12, 40–53.
- [4] Z.D. Stevanovic, E. Sieniawska, K. Glowniak, et al., *Front. Bioeng. Biotechnol.* 2020, 8, 563.
- [5] M.V. Dinu, A.C. Gradinaru, M.M. Lazar et al. *Int. J. Biol. Macromol.* 2021, 184, 898-908.

Acknowledgment:

The PN-III-P4-ID-PCE-2020-0296 project is gratefully acknowledged.

SYNTHESIS AND CHARACTERIZATION OF NOVEL IMINE DERIVATIVES OF QUATERNARY AMMONIUM SALT OF CHITOSAN

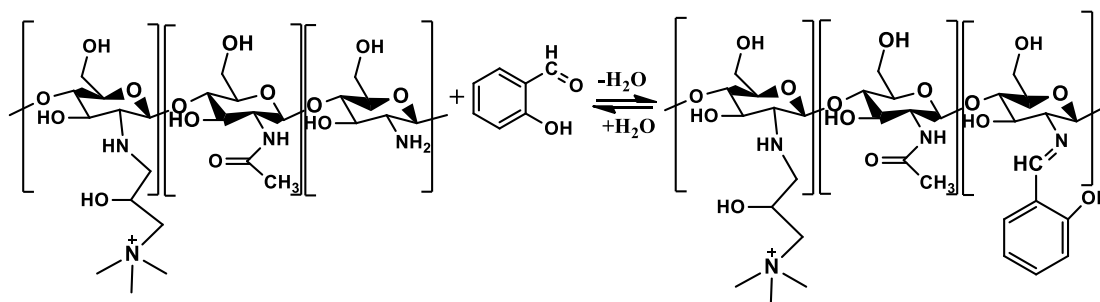
Bianca-Iustina Andreica*, Irina Rosca, Luminita Marin
Petru Poni Institute of Macromolecular Chemistry, Iasi, Romania
*andreica.bianca@icmpp.ro

Introduction

Crosslinking hydrophilic polymer chains by either chemical or physical linkages has led to the promising world of three-dimensional (3D) networks of hydrogels. Their remarkable properties, which attained striking attention regarding their use for various applications include biocompatibility, biodegradability, hydrophilicity, softness, superabsorbancy, and not only [1]. Among the polymers used for designing hydrogels, chitosan was highly exploited due to its abundance in nature and intrinsic properties. An important technique used for chitosan's hydrogelation was the reversible imination with natural monoaldehydes, which favoured the crosslinking by self-organization of the newly formed imine units into crosslinking nodes [2]. In this context, this work presents the synthesis and characterization of novel hydrogels obtained from a chitosan derivative crosslinked with salicylaldehyde. N-(2-hydroxy)propyl-3-trimethyl ammonium chitosan chloride (HTCC) was chosen on the grounds of its improved solubility in water and its antimicrobial properties which recommend its use for biomedical application [3].

Synthesis of hydrogels

The quaternary ammonium salt of chitosan (HTCC) was firstly synthesised by the ring-opening reaction of glycidyltrimethylammonium chloride with chitosan in heterogeneous system [4]. The chitosan derivative was fully characterized and its degree of quaternization was 43%, assessed by conductometric titration. The hydrogels were obtained from a 3% solution of HTCC in water, by slowly adding a 3% solution of salicylaldehyde in ethanol, under continuous stirring, at 55 °C (Scheme 1). A series of 15 hydrogels was obtained, by varying the ratio between amine groups of HTCC and aldehyde functionality of salicylaldehyde, from 1/1 to 15/1.



Scheme 1. Imination reaction of HTCC with salicylaldehyde

Characterization of the hydrogels

The hydrogels were firstly evaluated from the structural point of view, by ¹H Nuclear Magnetic Resonance and Fourier-Transformed Infrared Spectroscopy. Their supramolecular organization was confirmed by Wide-Angle X-Ray Diffraction and further analysed by Polarized Optical Microscopy. The morphology of the hydrogels was assessed using Scanning Electron Microscopy. The mass equilibrium swelling (MES) of the lyophilized hydrogels was evaluated in water and in different pH conditions. Moreover, preliminary investigation regarding the activity of the hydrogels against various microorganisms was evaluated.

Results and discussions

Fifteen hydrogels were obtained by acid condensation reaction between the amine groups of N-(2-hydroxy)propyl-3-trimethyl ammonium chitosan chloride and the aldehyde group of salicylaldehyde, by

varying the molar ratios of the NH_2/CHO functionalities. All the hydrogels passed the inverted tube test, regardless the molar ratios between amine and aldehyde functionalities used in their synthesis (Figure 1). The success of the imination reaction was confirmed by both NMR and FTIR spectroscopy. NMR spectra also suggested the reversibility of the imine linkage into hydrogels, by the concomitant presence of aldehyde and imine protons. On the other hand, the FTIR spectra indicated the completely shifting of the imination equilibrium to the products after removing water to obtain the corresponding xerogels.

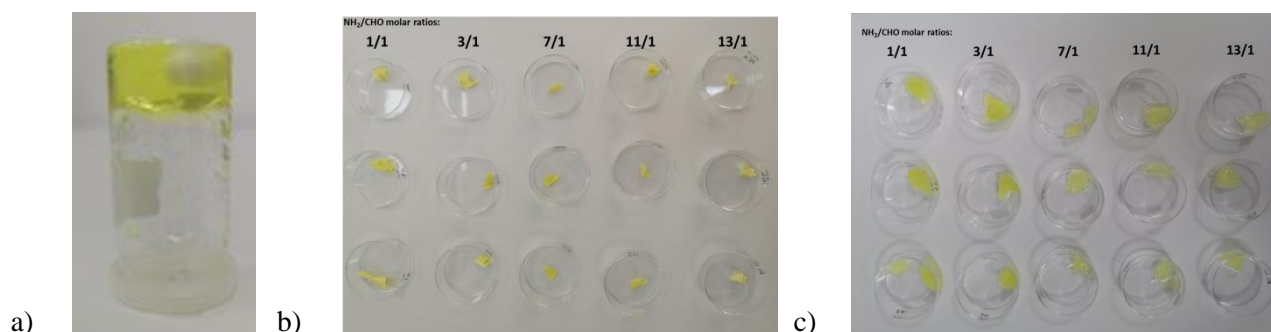


Figure 1. a) Inverted tube test of the hydrogel obtained for NH_2/CHO molar ratio of 7/1; b) Xerogels before immersing in water and c) Xerogels after immersing in water for 1 hour

WXR D diffractograms of the xerogels presented three reflexion bands, in agreement with a three-dimensional network. The information provided by WXR D was also confirmed by POM, the hydrogels possessing birefringence, indicating their ordering degree.

The xerogels completely rehydrated in water and buffer solutions of different pH (7.4 and 5.5) in less than one hour, and rapidly swelled reaching a mass equilibrium swelling in water of 230 after 24 hours.

Considering the approached synthetic strategy based on reversible imine linkage, the hydrogels proved to have self-healing ability after being cut in two pieces and being kept connected, at room temperature.

Preliminary investigation of the activity of hydrogels against common microorganisms proved promising results due to positive charge of the permanent positive charge of HTCC.

References

- [1] S. Bashir, M. Hina, J. Iqbal, A.H. Rajpar, M.A. Mujtaba, N.A. Alghamdi, S. Wageh, K. Ramesh, S. Ramesh, *Polymers*. 2020, 12.
- [2] M.M. Iftime, L. Mititelu-Tartau, L. Marin, *Int. J. Biol. Macromol.* 2020, 160, 398-408.
- [3] B.I. Andreica, X. Cheng, L. Marin, *Int. J. Biol. Macromol.* 2020, 139.
- [4] Y. Pakzad, M. Fathi, Y. Omid, M. Mozafari, A. Zamanian, *Int. J. Biol. Macromol.* 2020, 159, 117-128.

Acknowledgment:

This work was supported by a grant of the Ministry of Research, Innovation and Digitization, CNCS/CCCDI – UEFISCDI, project number PN-III-P4-ID-PCE2020-2717.

IMPROVED DOMAIN AND SELECTIVITY FOR URIC ACID DETECTION USING AS SENSITIVE MATERIALS COMPLEXES BETWEEN AN AMINO FUNCTIONALIZED PORPHYRIN AND CUNPs, PTNPs OR Pt@CuNP_s

Camelia Epuran*

Coriolan Dragulescu Institute of Chemistry, Timisoara, Romania

**camy.epuran@yahoo.ro*

Uric acid (UA) represented in Figure 1a is the primary and product of purine metabolism being present in a concentration range of 4.1 - 8.8 mg/100 mL in serum for normal, healthy humans [1]. Uric acid is present in the body in the form of urate, UA salt, and is excreted in the urine [2]. High levels of uric acid in the body cause diseases such as: high blood pressure, type 2 diabetes, gout [3].

Consequently, uric acid is considered an important biomarker in urine, serum and thus several studies have been developed for monitoring of high levels of uric acid by various detection techniques. The most performant technique that was used in the last years for the specific determination of uric acid was cyclic voltammetry offering the best detection limit of 6.0×10^{-7} mol/L⁻¹ [4].

Functionalized hybrid nanomaterials based on synergistic behavior given by an amino-substituted porphyrin, namely: 5, 10, 15, 20-tetrakis (4-amino-phenyl)-porphyrin, (TAmPP) complexed with CuNPs, PtNPs or core-shell Pt@CuNPs were used in optical detection of uric acid, and carefully compared from the point of view of selectivity, sensitivity and detection domain, with the purpose to finally select the best performing sensitive material. In Figure 1 there are presented SEM images of metal nanoparticles.

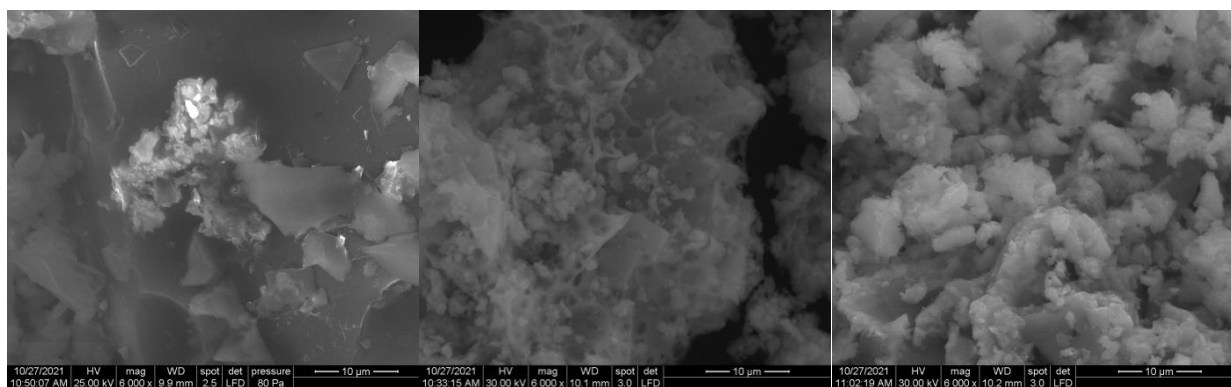


Figure 1. SEM images of CuNPs, PtNPs and core-shell Pt@CuNPs

A general conclusion is that the complexation of porphyrin with either of the tested metal nanoparticles is useful for increasing the detection range. A study of interference effects produced by species highly present in human serum and urine have been performed for: glucose (Glu), ascorbic acid (AA), NaCl, KCl, CH₃COONa, MgSO₄, KI, lactic acid (LA), sodium salicylate (SS) using concentrated solutions 1000 times higher than that of uric acid.

All the synthesized hybrid materials can be applied in the detection of uric acid in human fluids in a combined range between 0.5 µM- 15 µM concentrations, the best detection limit, that represents one of the most performant results reported in literature [3], being obtained by the porphyrin base alone. This result determines us to reconsider the detection mechanism.



References

- [1] T. Ting-Ting, H. Li, C. Sheng-Jie, Q. Wang, T. Qing-Wu, B.B. Zhang, J. Zhu, H. Guo-Wei, L. Li-Min, C. Xuan, *Dis. Markers*. 2018, 1–8.
- [2] J. Maiuolo, F. Oppedisano, S. Gratteri, C. Muscoli, V. Mollace, *Int. J. Cardiol.* 2016, 213, 8–14.
- [3] A. Abellán-Llobregat, L. Vidal, R. Rodríguez-Amaro, Á. Berenguer-Murcia, A. Canals, E. Morallón, *Electrochim. Acta.* 2017, 227, 275–284.
- [4] D. Lakshmi, M. J. Whitcombe, F. Davis, P. S. Sharma, B.B. Prasad, *Electroanalysis*, 2011, 23, 305–320.

Acknowledgment: The authors kindly thank for the support of Romanian Academy - Programme 3/2021 from Institute of Chemistry Timisoara.

BIODEGRADABLE IMINO-CHITOSAN NANOFIBERS AS WOUND DRESSING MATERIALS

Alexandru Anisiej,* Irina Rosca, Andreea-Isabela Sandu, Adrian Bele, Luminita Marin

Petru Poni Institute of Macromolecular Chemistry, Iasi, Romania

**anisiei.alexandru@icmpp.ro*

The aim of the study was the preparation and characterization of chitosan nanofibers with enhanced antimicrobial activity in view of application as wound dressings materials. The proposed materials were designed starting from chitosan, considering its large availability, biodegradability and bioactive properties. Moreover, the similarity of the chitosan nanofibers with the natural extracellular matrix, their high absorption capacity and high active surface to volume ratio, represented also important advantages considered for the development of wound dressing materials.

However, due to chitosan's poor solubility, neat fibers are difficult to be obtained. To overcome this drawback, the chitosan nanofibers were prepared by electrospinning with the aid of poly(ethylene oxide) in concentrated acetic acid solution, at room temperature, followed by the neutralization of the fibers and the washing of the poly(ethylene oxide) with ultrapure water, in order to obtain pure chitosan nanofibers. Even though chitosan is known in the literature as presenting antimicrobial activity, mainly in solution, for wound dressing applications is required a high antimicrobial activity in solid state. That is why, chitosan nanofibers were modified by imination with a monoaldehyde, known for its high antimicrobial activity, 2-formylphenilboronic acid [1, 2]. The imination reaction was performed in heterogenous system in different molar ratios of reagents' functionalities, leading to functionalized nanofibers with various aldehyde contents (Figure 1).

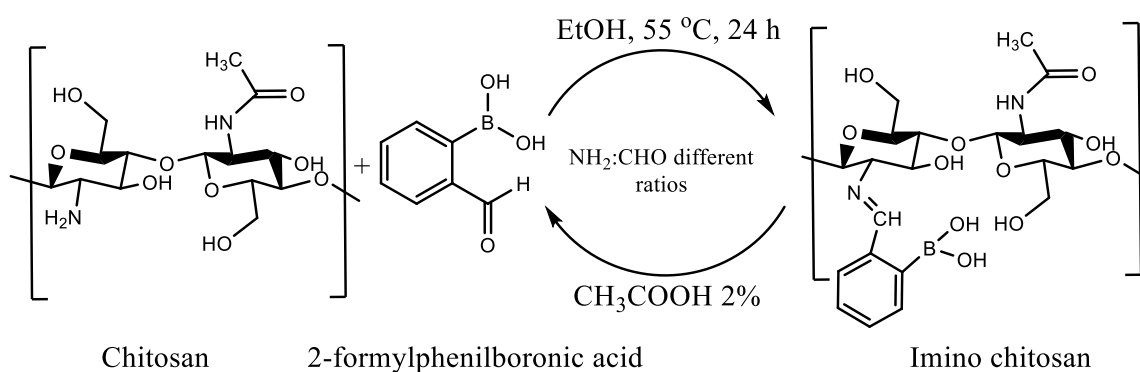


Figure 1. Imination of chitosan fibers with the antimicrobial aldehyde in heterogeneous system

The infrared spectroscopy (FTIR) and proton nuclear magnetic resonance spectroscopy (¹H-NMR) confirmed the successful imination of the nanofibers by the appearance of the signals corresponding to the newly formed imine linkages. The morphology, crystallinity, porosity and intermolecular forces of the modified fibers were further studied by scanning electron microscopy (SEM), polarized light microscopy (PLM), dynamic vapor sorption (DVS) and thermogravimetric analysis (TGA) techniques. To evaluate the potential of these materials in wound healing applications, the obtained fibers were subjected to swelling and biodegradation tests both in water and PBS, as well as antimicrobial and biocompatibility test. Nanofiber swelling showed high mass equilibrium swelling values, reaching a maximum of 30 in water, in agreement with the requirements for wound dressing applications. The biodegradability tests, performed in the presence of



lysozyme, indicated high mass loss values due to both hydrolytic and enzymatic degradation of the nanofibers. Moreover, the biodegradation rate in media of different pH fitted well the evolution of exudate pH over wound healing period, indicating their total biodegradation up to total healing. The evaluation of the antimicrobial activity of the iminoboronate nanofibers, performed using the Kirby Bauer method, led to high values of the diameter of the inhibition zones, while the cytocompatibility tests on normal human fibroblasts revealed good biocompatibility for an imination degree around 15 %.

All these findings indicated these new materials as potential biodegradable wound dressing materials.

References

- [1] A. Moeini, P. Pedram, P. Makvandi, M. Malinconico, G. Gomez d' Ayala, *Carbohydr. Polym.* 2020, 233, 115839;
- [2] D. Ailincăi, L. Marin, S. Morariu, M. Mares, A.-C. Bostanaru, M. Pinteala, M. Barboiu, *Carbohydr. Polym.* 2016, 152, 306–316.

Acknowledgment: This work was supported by a grant of the Ministry of Research, Innovation and Digitization, CNCS/CCCDI–UEFISCDI, project number 538PED/2020 within PNCDI III.

NOVEL LUMINESCENT PHENOTHIAZINE DERIVATIVES FOR BIOLOGICAL APPLICATIONS

Sandu Cibotaru,* Luminita Marin

Petru Poni Institute of Macromolecular Chemistry, Iasi, Romania

**cibotaru.sandu@icmpp.ro*

Phenothiazine derivatives are well-known for their wide applicability in different fields. Due to the electron rich sulfur and nitrogen heteroatoms from the phenothiazine core and its butterfly geometry, they are used as building blocks to design materials for high performance electronic and optoelectronic devices including light-emitting diodes, photovoltaic cells, thin film transistors, and electro-chromic devices [1-3]. The photoluminescence of the phenothiazine based compounds can be easily tuned by modifying the chemical structure of the phenothiazine core, especially by adding an acceptor moiety or a chromophore [4]. Phenothiazine derivatives are also known for their biological activity as analgesic, antipsychotic, immunosuppressive, anti-inflammatory, bactericide, fungicide and anticancer [5]. These properties are further enriched by combining the phenothiazine core with other bioactive moieties, when new multifunctional compounds are obtained [6].

In this context, the present study aimed to synthesize bioactive phenothiazine derivatives containing sulfonamide moiety, for biomedical applications including biological imaging. Therefore, a series of four phenothiazine based imines and two corresponding aldehydes were synthesized by chemical modification of a phenothiazine core containing a poly(ethylene glycol) (PEG) chain at the nitrogen atom or triethylene glycol (TEG) chain, respectively (Scheme 1). The aldehydes were synthesized by Vilsmeier reaction, and they were further transformed into imines by the condensation reaction with two different sulfonamides under microwave irradiation.

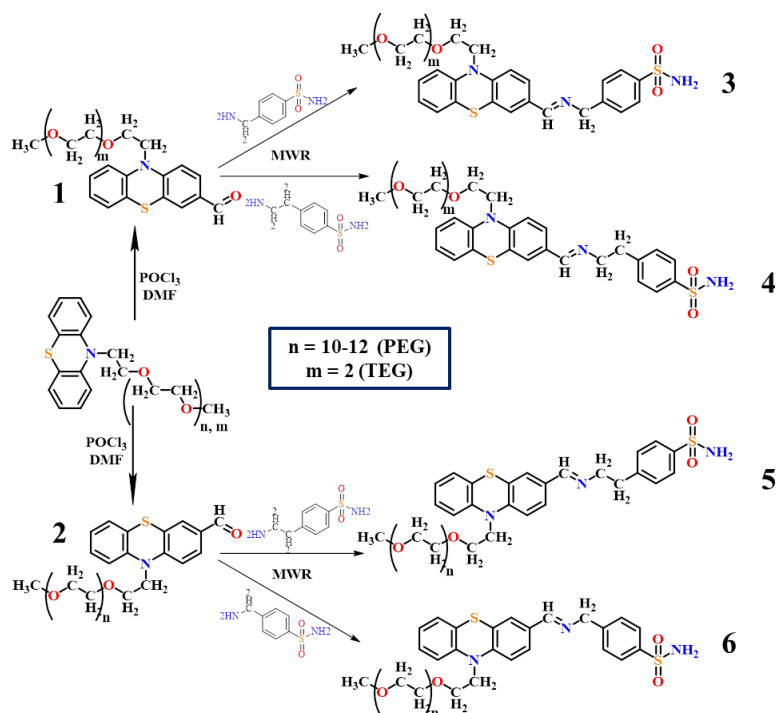


Figure 1. Compound 1 under UV light

Scheme 1. Synthetic pathway of the studied compounds

¹H and ¹³C NMR and FTIR spectroscopy confirmed the successful formylation of the phenothiazine core (compounds **1** and **2**) by the presence of the corresponding chemical shift and absorption bands, respectively, characteristic to the newly formed aldehyde unit. The high degree of purity of the compounds was demonstrated by the right ratio of the integrals corresponding to the aldehyde proton and aromatic protons from the phenothiazine core. Further, the successful imination of the **1** and **2** aldehydes was confirmed by NMR and FTIR spectroscopy, by the occurrence of characteristic chemical shift of imine proton at 8.41 ppm and characteristic vibrational band at 1644 cm⁻¹ respectively.

The photophysical behavior of the synthesized compounds has been studied by UV-vis and photoluminescence spectroscopy in three different solvents to highlight the solvent influence on emission properties of the compounds. By analyzing the obtained data, it was concluded that the compounds presented a solvatochromic effect. The quantum yield was measured using an integrated sphere, in all the solvents, reaching a maximum value of **51.72 %** for the sample **1**. An image of this solution is presented in **Figure 1**. Quite high values were obtained for the quantum yield also in solid state, revealing the versatility of these compounds, presenting potential also for optoelectronic applications.

The stability of the imine derivatives was checked using ¹H-NMR spectroscopy by recording the NMR spectra at three different moments during 13 days and two different DMSO:PBS ratios. The results indicated that, due to the water presence, an equilibrium between the reagents and the imine products is established, allowing to the formyl phenothiazine and sulfonamide parts to exhibit their biological activities, while maintaining the luminescent properties.

The biologic activity of the studied compounds, in terms of *in vitro* antimicrobial activity and biocompatibility, is under investigation. In view of *in vivo* applications, the biocompatibility will be assessed by monitoring the viability of the normal human fibroblasts in contact with the compounds solutions of different concentrations.

References:

- [1] E. A. Onoabedje, S. A. Egu, M. A. Ezeokonkwo, C. U. Okoro, *J. Mol. Struct.* 2019, 1175, 956-962.
- [2] P. Rajakumar, R. Kanagalatha, *Tetrahedron Lett.* 2007, 48, 8496–8500.
- [3] S. N. Al-Ghamdiab, H. A. Al-Ghamdic, R. M. El-Shishtawyad, A. M. Asiriae, *Dyes Pigm.* 2021, 194, 109638.
- [4] Y. Rout, C. Montanari, E. Pasciucco, R. Misra, B. Carlotti, *J. Am. Chem. Soc.* 2021, 143, 26, 9933–9943.
- [5] K. Pluta, B. Morak-Młodawska, M. Jeleń, *Eur. J. Med. Chem.* 2011, 46, 3179–3189.
- [6] M. M. Ghorab, M. S. Alsaid, N. Samir, G. A. Abdel-Latif, A. M. Soliman, F. A. Ragab, D. A. Abou El Ella, *Eur. J. Med. Chem.* 2017, 134, 304-315.

Acknowledgment: This work was supported by the a grant of the Ministry of Research, Innovation and Digitization, CNCS/CCCDI – UEFISCDI, project number PN-III-P4-ID-PCE2020-2717

XANTHAN AS COMPONENT OF THE DRUG DELIVERY SYSTEMS

Alexandra Dimofte,* Narcis Anghel, Maria Valentina Dinu, Iuliana Spiridon

Petru Poni Institute of Macromolecular Chemistry, Iasi, Romania

**dimofte.alexandra@icmpp.ro*

Introduction

Polysaccharides have widespread pharmaceutical applications, and nowadays they are increasingly used as biomaterials for drug delivery [1]. The aim of this study was to create a new drug delivery systems based on alginate (Alg), xanthan (Xa)/chemical modified xanthan (XaAO) with possible uses in the topical application. Piroxicam (P) and ketoconazole (K) were selected as model drugs and added into the polysaccharide matrix.

Experimental

Esterification of xanthan with oleic acid was performed at room temperature, *via* organic acid tosylate. The reaction product (XaAO) was separated by filtration and dried at room temperature. FTIR and ¹H-NMR spectra evidenced that the esterification reaction of xanthan took place.

New materials comprising equal amounts of polysaccharides (named Xa-Alg and XaAO-Alg), 0.05 g of piroxicam (Xa-Alg-P, XaAO-Alg-P), 0.05 g of ketoconazole (Xa-Alg-K, XaAO-Alg-K) and 0.1 g of piroxicam and ketoconazole, respectively (Xa-Alg-PK, XaAO-Alg-PK) were obtained by freeze-thawing cycles, followed by lyophilization. Obtained materials were characterized through FTIR (Bruker FTIR Spectrophotometer Vertex 70 - Billerica, MA, USA - equipped with an attenuated total reflection device), and Scanning Electron Microscopy (SEM—Quanta 200 instrument). Mechanical properties were evaluated by a Shimadzu Testing Machine EZ-LX/EZ-SX Series, Kyoto, Japan.

Results and discussion

The peaks at 1180cm⁻¹, 1529 cm⁻¹ (piroxicam) [2] and 2923 cm⁻¹, 1238 cm⁻¹ (ketoconazole) [3] in FTIR spectra confirm the presence of drugs in the obtained materials (Figure 1).

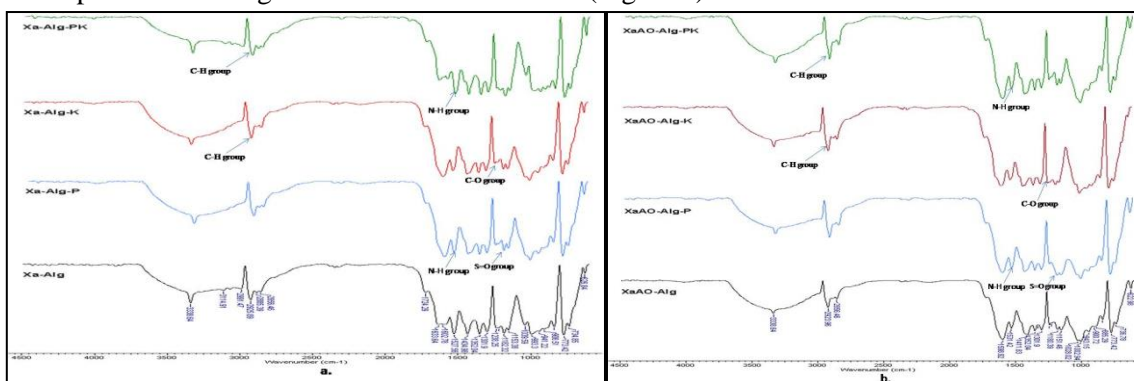


Figure 1. FTIR spectra for materials based on Xa-Alg (a) and XaAO-Alg (b) containing piroxicam and ketoconazole

When piroxicam was added into the Xa-Alg matrix, the resulted films recorded lower compressive strength (47.16%), with diminished elongation at the break point (Table 1). It seems that the interactions between the piroxicam and the polysaccharide matrix, at the concentration included into the formed gel network, reduced the intramolecular space inside the backbone, increasing the elasticity of the material [4]. When K was added into XaAO-Alg matrix, an increment of 54.14% in the compressive strength, as compared to that of Xa-Alg-K system, was registered. The same trend was kept when both piroxicam and ketoconazole were added into the XaAO-Alg matrix, an increment of 53.28% being recorded.

Table 1. Mechanical properties of materials

Sample	Elastic Modulus*, kPa	R ²	Compressive nominal stress**, kPa	Strain%
<i>Xa-Alg</i>	86.81	0.975	52.47	40.59
<i>Xa-Alg-P</i>	20.21	0.974	27.72	72.51
<i>Xa-Alg-K</i>	2.89	0.985	66.34	66.68
<i>Xa-Alg-PK</i>	3.12	0.992	29.19	81.68
<i>XaAO-Alg</i>	1.30	0.997	22.40	79.14
<i>XaAO-Alg-P</i>	9.28	0.998	37.83	68.39
<i>XaAO-Alg-K</i>	5.99	0.996	36.39	81.45
<i>XaAO-Alg-PK</i>	3.12	0.995	62.49	80.94

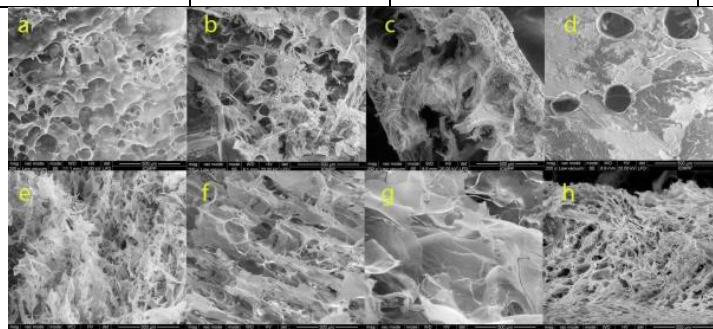


Figure 2. SEM images for Xa-Alg (a), Xa-Alg-P (b), Xa-Alg-K (c) and Xa-Alg-PK (d), XaAO-Alg (e), XaAO-Alg-P (f), XaAO-Alg-K (g) and XaAO-Alg-PK (h)

SEM images (Figure 2) evidence the formation of pores in all materials (studies related to the average pore size are in progress). The release of drugs from materials is best described by the Korsmeyer-Peppas model [5]. P and K are released at a slightly faster rate from the material based on Xa (Figure 3), compared with that comprising XaAO.



Figure 3. Drug release profile polysaccharides-based matrix (Xa-Alg (a) and XaAO-Alg (b))

Conclusions

New drug delivery systems based on polysaccharides-based matrix have been developed and characterized. FTIR spectra showed the presence of drugs in the materials. The compressive strength recorded an increase after loading of drugs into the XaAO-Alg matrix. The release kinetics of drugs fitted well the Korsmeyer-Peppas model, with non-Fickian and Fickian diffusion, depending on the composition of the polymeric matrix.

References

- [1] H. Yadav, C. Karthikeyan, Polysaccharide carriers for drug delivery, Ed. Woodhead Publ., Cambridge, 2019.
- [2] V. Nikolic, S. Ilic-Stojanovic, L. Nikolic, M. Dobrivoje Cakic, *Hem. Ind.* 2014, 68, 107-116.
- [3] P. Papneja, M. Kumar, A. Bilandi, *Eur. J. Pharm. Med. Res.* 2015, 2, 990-1014.
- [4] M. Tako, T. Teruya, T. Tamaki, *Colloid. Polym. Sci.* 2010, 288, 1161–1166.
- [5] M. L. Bruschi, Strategies to modify the drug release from pharmaceutical systems, Ed. Woodhead Publishing, Cambridge, 2015, p. 63-86.

ROBOSAMPLE: ROBOTICS-BASED GIBBS SAMPLING OF MACRO-MOLECULAR SYSTEMS

**Teodor Asvadur Sulea,* Eliza Cristina Martin, Victor Gabriel Ungureanu,
Laurențiu Spiridon, Andrei-Jose Petrescu**

*Department of Bioinformatics and Structural Biochemistry,
Institute of Biochemistry of the Romanian Academy, Bucharest, Romania
teodor.sulea@biochim.ro

Although ~10000 biomolecular structures are released every year, describing their free energy surfaces in particular thermodynamic states remains challenging in as much as it is paramount to understanding a wide range of biomolecular phenomena from protein folding to inter-molecular interactions. We present here **ROBOSAMPLE**, a software platform based on robotics, which lowers the difficulty of the task by employing Constrained Dynamics Hamiltonian Monte Carlo (CDHMC) coupled with Gibbs sampling. [1]

Molecular dynamics and Markov Chain Monte Carlo (MCMC) are two widely used methods for sampling molecular conformational spaces, both with their strengths and weaknesses. Molecular dynamics can reach distant basins but they are limited by the integration step and may introduce errors due to the numerical integration. Markov Chain Monte Carlo preserve exactly the Boltzmann distribution by using the Metropolis-Hastings criteria, but there are limited by the extent of the trials. Robosample implements both methods through a Hybrid/Hamiltonian Monte Carlo procedure which is an MCMC method that proposes its moves by molecular dynamics, and leads to highly uncorrelated samples.

The novelty of Robosample when compared to other HMC methods is the usage of constraints at certain time intervals on hard degrees of freedom that transform in rigid bodies various parts of the modelled molecule, without sacrificing computing time on calculating Lagrange multipliers equations in a Cartesian coordinates stage. This is only possible in reduced generalized coordinates, with algorithms previously developed by roboticists. More precisely, constrained momenta marginalization is required to preserve the Boltzmann distribution, and comes with the addition of two new factors: the determinant of the mass metric tensor and its square root. In the general case, both calculations would have an N^3 complexity, but they were solved linearly (N complexity) due to the matrix special internal structure using algorithms in the field of robot mechanics [2]. The algorithms are implemented in Robosample.

Robosample simulations don't use only constrained dynamics, but they also mix constrained moves with fully flexible moves through the means of Gibbs sampling therefore achieving ergodicity and recovering the full conformational space [3].

Given this setting, in this work we aimed to unleash the true power of robot mechanics developments, such as the introduction of different type of joints apart from the torsional one (Pin) which was the main one used before (see figure 1). Hence, we implemented and tested two new joint types: Ball and Cylinder with 3 and 2 degrees of freedom respectively. The first one combines the torsional and angular movements while the second combines the bond sliding motion with the torsional and both correctly reproduce the alanine dipeptide free energy surface. Cylinder joint simulations were able to achieve faster free energy surface convergence than the torsional ones however not as fast as the Ball ones with C5 to aL mean first passage times of 615 and 518 molecular dynamics steps respectively. Molecular dynamics moves were tuned at different time steps in order to achieve the same acceptance rate at around ~0.65.

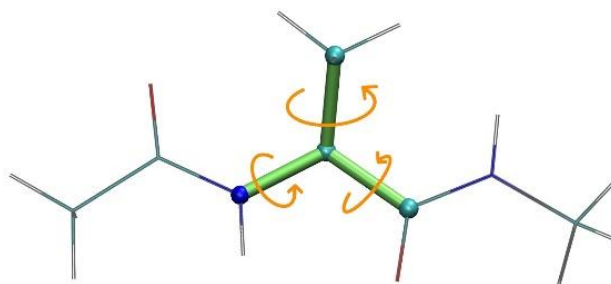


Figure 1: Alanine Dipeptide molecule, with flexible joints shown in green and constrained parts outlined in grey. Orange arrows show the direction the pin-type joints can move.

Generated in VMD v.1.9.4

ROBOSAMPLE is also user-friendly, equipped with a python interface that allows any user to define many types of constraints, having little prior knowledge on the energetics of the system. Flexibility can be automatically defined using structural, functional or physico-chemical properties of the molecule, such as secondary structure, Solvent Accessible Surface Area or particular stretches of aminoacids (i.e. a binding site). The entire software package is open-source and freely downloadable at <https://github.com/spirilaurentiu/Robosample>.

Robosample offers a new way of doing molecular simulations which do not exclude the coupling with other enhanced sampling methods. This can lead to significant improvement in computer time used to understand a particular molecular phenomenon. Apart from its intrinsic fundamental importance for knowledge, this type of insight is also most of the times, translated in key applications for biomedical, biotechnological or agricultural fields.

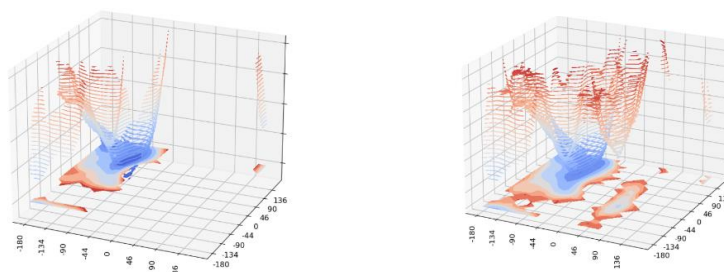


Figure 2: 3D Contour maps of the Free Energy Surface. Left: Using Pin-Type joints; Right: Using Ball-Type Joints. Image generated using Matplotlib v. 3.4.3

References

- [1] L. Spiridon, TA Șulea, DDL. Minh, AJ Petrescu, *Biochim Biophys Acta Gen Subj*, 2020, 8.
- [2] G. Rodriguez & Jet Propulsion Laboratory (U.S.), *National Aeronautics and Space Administration*, 1986.
- [3] L. Spiridon, DDL. Minh, *J Chem Theory Comput.* 2017, 13, 4649-4659.

Acknowledgment: This work was supported by a grant of the Romanian Ministry of Education and Research, CNCS - UEFISCDI, project number PN-III-P4-ID-PCE-2020-2444, within PNCDI III

IONIC BEADS/ CaCO_3 COMPOSITES AS SORBENTS FOR SMALL ORGANIC MOLECULES

Ana-Lavinia Vasiliu*, Marius-Mihai Zaharia, Marcela Mihai

Petru Poni Institute of Macromolecular Chemistry, Iasi, Romania

**vasiliu.lavinia@icmpp.ro*

Introduction

Due to their nonbiodegradability, high toxicity, and carcinogenic effect, organic materials such as dyes and residual drugs are regarded particularly dangerous to the environment [1]. With an ever-increasing global demand for water, removing harmful contaminants remains a constant challenge [2]. Due to their porous multi-channeled structure and electrostatic and steric effects [3], ion exchange resins have sorption properties [4]. Calcium carbonate is a widely used biomineral, with proven ability to sorb different dyes [5], heavy metal ions [6] and drugs [7]. Herein, composite CaCO_3 /ionic beads composites were obtained and their ability to sorb dyes (neutral red, NR, and bromocresol green, BCG) and drugs (tetracycline, TCH) was investigated.

Experimental

The ion exchanger beads (IEx) obtained from the copolymer divinylbenzene/ethyl acrylate/acrylonitrile, functionalized with anionic groups (by introducing COOH groups, IExCOOH), cationic groups (with amino groups introduced by aminolysis with ethylenediamine, IExEDA) and zwitterionic groups (by carboxymethylation reaction performed on the weak cationic ion exchangers, IExZw) were used as substrate for the CaCO_3 crystallization. The IEx samples were placed in Petri dishes with CaCl_2 solutions and kept in a desiccator having NH_4HCO_3 as carbonate source, for 5 days. The resulting composites were characterized by SEM, XRD and EDX. The sorption capacity of the samples was evaluated by UV-Vis, by measuring the absorbance of the supernatant at 615 nm for BCG and 276 nm for NR and TCH. The TCH release was conducted in phosphate buffer solution, pH 7.4, for 72 hours, at a constant temperature of 37°C.

Results and discussions

The CaCO_3 crystallization on the IEx led to a decrease of the beads surface roughness, obtaining a smooth and compact surface, with almost no large crystals, most probably due to the affinity of acidic functional groups to Ca^{2+} ions which act as crystallization seeds, making the carbonate ions easier to be fixed in the crystal lattice (Figure 1).

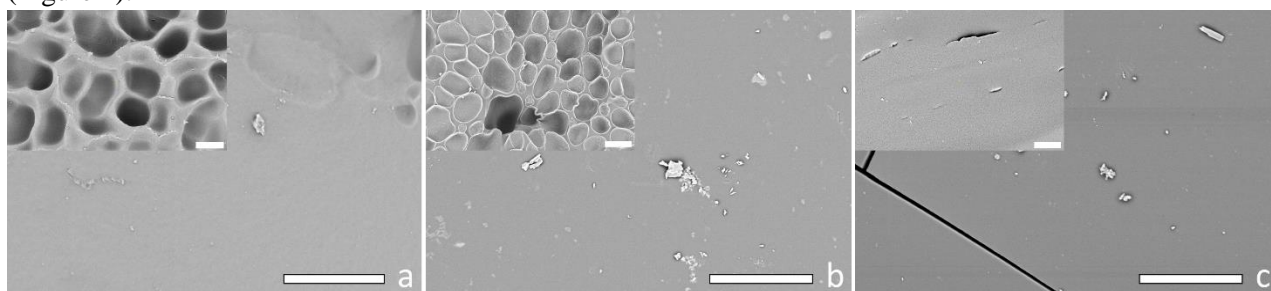


Figure 1. SEM images of IEx/ CaCO_3 composites with anionic (a), cationic (b) and amphoteric (c) functional groups; insets of IEx initial surface (10 μm scale bar in all images).

The sorption capacity (S_c) of the beads and corresponding composites for BCG, NR and TCH is summarized in Table 1. The anionic samples do not adsorb the BCG dye, due to the presence of anionic functional groups both in the dye and in the samples, which leads to electrostatic repulsions. The amphoteric samples showed an increase of S_c due to the presence of both anionic and cationic functional groups. The cationic samples showed very good S_c values due to the presence of oppositely charged functional groups in the dye and in the

investigated samples. The CaCO₃ crystallization on the beads did not significantly influence the sorption capacity of the BCG dye.

The cationic samples showed lower S_C values for the NR dye, as compared to the anionic and amphoteric ones. The CaCO₃ crystallization on the beads increased their sorption capacity, which means that the sorption mechanism is influenced by both electrostatic interactions between the dyes and the polymeric matrix functional groups and also by the CaCO₃ crystals capacity to interact with the dye, as proven by a previous study [8].

Table 1. Sorption capacity of the beads and corresponding composites

Sample	BCG S _C , mg/g		NR S _C , mg/g		TCH S _C , mg/g	
	IE _x	IE _x /CaCO ₃	IE _x	IE _x /CaCO ₃	IE _x	IE _x /CaCO ₃
IE _x COOH	0.004	0.005	2.207	2.288	11.958	17.908
IE _x EDA	2.176	2.198	0.268	0.210	50.247	41.611
IE _x Zw	0.566	0.465	1.688	2.234	11.988	36.193

All of the investigated samples presented a significantly higher S_C for TCH, the highest value being in the case of cationic samples, as compared to the anionic and amphoteric ones. The IE_x/CaCO₃ composites showed an increase of the S_C for TCH, due to the synergetic contribution of several factors: the polymeric matrix ability to adsorb TCH by electrostatic bonds, the availability of functional groups after the CaCO₃ growth, the distribution of the CaCO₃ crystals on the samples and the crystals ability to interact with TCH. The TCH release profiles show a very fast drug release after only 2 minutes of immersion, with a drug release degree up to 37.7% in the case of anionic sample, which can be ascribed to the slow diffusion of the drug found at the samples surface. Then, a gradual release behavior is observed, that extended up to 15 hours, until the equilibrium was reached. The CaCO₃ presence in the beads led to a slower drug release. The anionic sample showed the fastest drug release, the time for reaching the maximum amount released being 140 minutes.

References

- [1] T. Rasheed, S. Shafi, M. Bilal, T. Hussain, F. Sher, K. Rizwan, *J. Mol. Liq.* 2020, 318, 113960.
- [2] M.F. Hanafi, N. Sapawe, *Mater. Today: Proceedings* 2021, 31, A158-A165.
- [3] M. El Hefnawy, A.F. Shaaban, H.A. El Khawaga, *J. Environ. Chem. Eng.* 2020, 8, 103788.
- [4] S.D. Alexandratos, *Ind. Eng. Chem. Res.* 2009, 48, 388-398.
- [5] M. Zhao, Z. Chen, X. Lv, K. Zhou, J. Zhang, X. Tian, X. Ren, X. Mei, *R. Soc. Open Sci.* 2017, 4, 170697.
- [6] I. Bunia, V. Socoliuc, L. Vekas, F. Doroftei, C. Varganici, A. Coroaba, B.C. Simionescu, M. Mihai, *Chem. Eur. J.* 2016, 22, 18036-18044.
- [7] J. Wang, J.-S. Chen, J.-Y. Zong, F. Li, R.-X. Zhuo, S.-X. Cheng, *J. Phys. Chem. C* 2010, 114, 18940-18945.
- [8] M. Mihai, F. Doroftei, A.-L. Vasiliu, I. Bunia, *Rev. Roum. Chim.* 2017, 62, 499-504.

Acknowledgment: This work was supported by grants of the Ministry of Research, Innovation and Digitization, CNCS/CCCDI – UEFISCDI, project number PN-III-P1-1.1-PD-2019-0286 and project number PN-III-P4-ID-PCE-2020-1541, within PNCDI III.

EFFICIENT RECOVERY OF WASTEWATERS BASED ON BENEFICIAL INTERFERENCES BETWEEN PORPHYRIN DERIVATIVES, PLATINUM NANOPARTICLES AND SILICA MESOPOROUS MATRICES

Ion Fratilescu

Coriolan Dragulescu Institute of Chemistry, Timisoara, Romania
ion.fratilescu@gmail.com

Wastewater containing dyes is still a major problem that threatens the ecological balance of aquatic ecosystems, due to the residual toxicity and resistance of dye molecules to biodegradation. Although many toxic dyes such as Congo red or malachite green may be banned in European Union countries or United States of America, they are still used in many countries around the world [1,2,3].

A set of hybrid materials based on mesoporous silica functionalized with either solely Pt(II)-5,10,15,20-tetrakis[4-(2-propen-1-yloxy)phenyl]porphyrin (Pt-TAOPP) or platinum nanoparticles (PtNPs) or with both porphyrin base 5,10,15,20-tetrakis[4-(2-propen-1-yloxy)phenyl]porphyrin (TAOPP) and PtNPs, were obtained and fully characterized by UV-vis, FT-IR, BET, AFM to put into evidence the improvements of optical, topographical and morphological properties. Functionalized mesoporous silica nanomaterials were synthesized applying a two-step acid-base catalyzed sol-gel process utilizing tetraethoxysilane (TEOS) as silica source precursor, as schematically presented in Figure 1 for silica nanomaterial incorporating Pt-TAOPP [4].

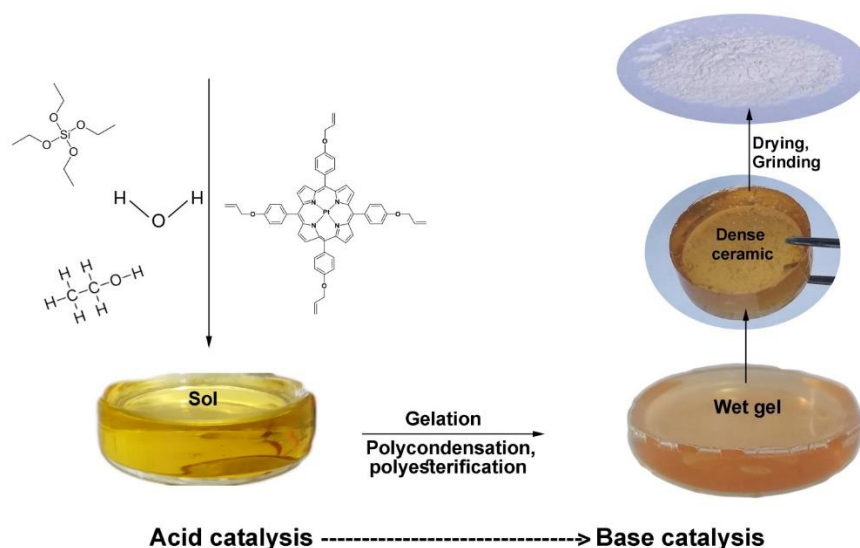


Figure 1. Scheme for obtaining the silica nanomaterial, by acid-base catalysis in two steps with *in situ* incorporation of Pt-TAOPP

Testing the ability to remove dyes from aqueous solutions was performed in glass test tubes with equally amounts of absorbent material from all 3 functionalized silica and control silica with a loading of 3.3 g / L. Absorption spectra of dye solutions were performed before and after treatment with nanomaterials (after filtration).

The results are obvious even with the naked eye after only 2.5 hours as can be seen in Figure 2, where the functionalized silica materials were tested with 5×10^{-5} M initial concentration solutions of Congo Red.







Adsorbent	Congo red 5×10^{-5} M	
	Initially	After 160 min
(TAOPP-PtNPs) -silica hybrid		
PtTAOPP -silica hybrid		
PtNPs -silica hybrid		

Figure 2. Discoloration of Congo Red solution on different functionalized silica functionalized matrices

All of the hybrid silica nanomaterials work well in removing dyes, achieving yields between 73 and 100%. [5].

References

- [1] M. Hernández-Zamora, F. Martínez-Jerónimo, *Environ. Sci. Pollut. Res.* 2019, 26, 11743-11755
doi:10.1007/s11356-019-04589-1
- [2] L.H. Ahlström, C. Sparr Eskilsson, E. Björklund, *Trends Anal. Chem.* 2005, 24 49-56.
doi:10.1016/j.trac.2004.09.004
- [3] J. Schmit, C. MacLeod, E. Weise, B. Hansen, [Chinese fish crisis shows seafood safety challenges](#), *USA Today*, 7/1/2007
- [4] D. Anghel, A. Lascu, C. Epuran, I. Fratilesco, C. Ianasi, M. Birdeanu, E. Fagadar-Cosma, *Int. J. Mol. Sci.* 2020, 21, 4262. doi:10.3390/ijms21124262
- [5] I. Fratilesco, Z. Dudás, M. Birdeanu, C. Epuran, D. Anghel, I. Fringu, A. Lascu, A. Len, E. Fagadar-Cosma, *Nanomaterials*. 2021, 11, 863. doi:10.3390/nano11040863

Acknowledgment: The author gratefully acknowledges the help of the "Coriolan Drăgulescu" Institute of Chemistry - Program 3 and funding from UEFISCDI-FET Project 76 PCCDI/2018, ECOTECH-GMP and UEFISCDI-FET Project 76 PCCDI/2018.

COMPOSITE MATERIALS BASED ON POLYELECTROLYTES - SORBENTS IN BATCH AND COLUMN STUDIES

Larisa-Maria Petrila,* Florin Bucatariu, Marcela Mihai
Petru Poni Institute of Macromolecular Chemistry, Iasi, Romania
**larisa.petrila@icmpp.ro*

Since the introduction of the layer-by-layer (LbL) deposition model by Iler in the 1960s [1] and its development by Decher and Hong in the 1990s [2], the deposition of multilayers based on polyelectrolytes have emerged as an effective method of modifying surfaces, regardless of their shape and nature. The deposition of polyelectrolyte multilayers can be performed on flat or three-dimensional templates, allowing the fabrication of materials with various properties. Composite materials obtained by LbL deposition of polyelectrolytes on inorganic substrates are versatile materials, characterized by high stability, large number of functional groups and tunable properties [3]. Polyelectrolyte-based multilayers have found numerous applications in top fields of science: drug-controlled release systems, tissue engineering, biosensor production, environmental remediation and pollutant retention, and the development of modern energy conversion and storage systems [4]. To date, a large number of emerging pollutants were separated from polluted water using composite materials based on polyelectrolyte multilayers [5,6], demonstrating the applicability of this sorbents in wastewater treatment.

The study was focused in the synthesis and characterization of composite materials obtained by LbL deposition of linear and branched poly(ethyleneimine) (PEIL and PEIB) and poly(acrylic acid) (PAA) on silica microparticles. The deposition of polyelectrolytes on the silica substrate was performed until 2.5 and 4.5 polycation/polyanion bilayers have been deposited. The multilayers were chemically cross-linked with glutaraldehyde and the PAA chains were removed (extracted) in strong basic media, obtaining Daisogel/(PEI)₃ și Daisogel/(PEI)₅ composites. The scanning electron microscopy (SEM), and Energy-Dispersive X-ray Analysis (EDAX) results are shown in Figure 1.

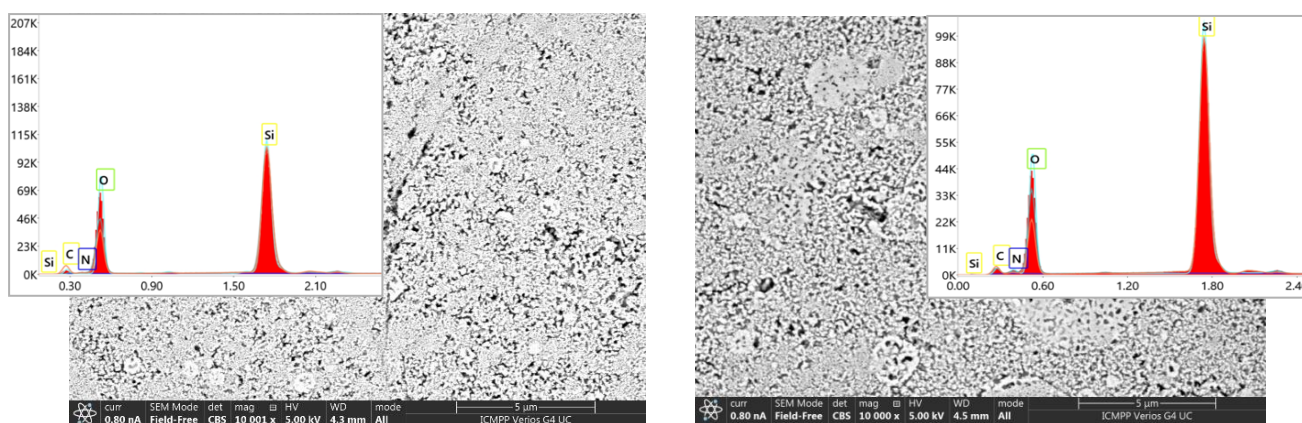


Figure 1. SEM and EDAX results for (PEIB)₃ (left) and (PEIB)₅ composites (right)

The obtained composites were used in sorption experiments in batch and column, using gallic acid (GaAc) as a negatively charged model pollutant. To evaluate the capacity of the composite microparticles for the GaAc sorption, a series of batch and column experiments have been carried out before and after the extraction of PAA chains from cross-linked polycation chains (Figure 2).

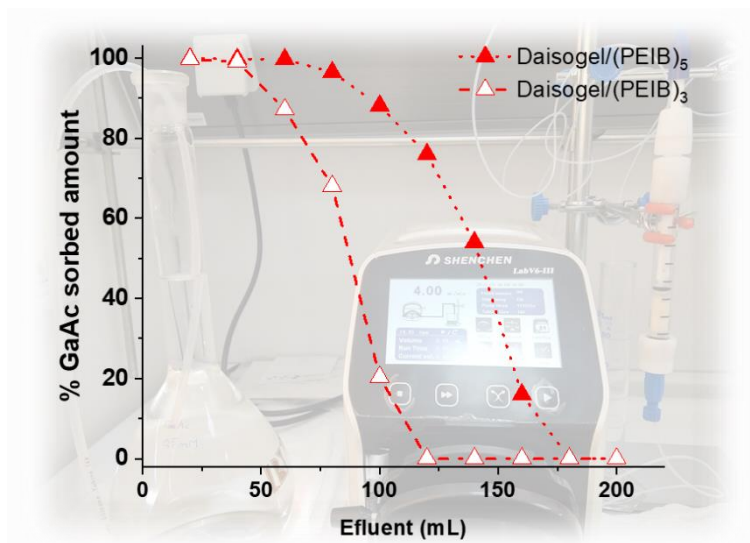


Figure 2. Column sorption of GaAc onto Daisogel/(PEIB)_n composites

The non-extracted microparticles retained lower quantities of GaAc mainly due to the electrostatic repulsions between carboxylic groups of GaAc and the carboxylic groups of PAA. The best results were obtained with the extracted microparticles where a larger number of polycation amino groups are more accessible to the anionic charged molecules. The highest sorbed amount of GaAc was recorded by the Daisogel/(PEIB)₅ microparticles (~30 mg/g) as a result of a higher stability of PEIB chains in basic media during the PAA extraction. The column experiments demonstrated that the sorption capacity of each composite depended on the shell organic amount. The multiple sorption/desorption cycles of GaAc carried out in dynamic conditions without losing the sorption capacity in each cycle, demonstrated the reusability of these composite materials in sorption of anionic species dissolved in water. Based on the experimental data obtained in batch and dynamic experiments, it was demonstrated that solid core/shell sorbents based on silica and polycations interact mainly electrostatically with the anionic weakly charged GaAc molecules.

The column and batch experiments demonstrated that extracted composite materials are stable and present higher sorption capacities for GaAc, compared with the non-extracted materials. The multiple sorption/desorption studies demonstrated the reusability of the composite materials and their potential use in removing anionic charged organic molecules dissolved in aqueous solutions.

References

- [1] R.K. Iler, *J. Colloid Interface Sci* 1966, 21(6), 569-594
- [2] G. Decher, J.D. Hong, J. Schmitt, *Thin Solid Films* 1992, 210-211
- [3] I.S. Elizarova, P.F. Luckham, *Adv. Colloid Interface Sci.* 2018, 262, 1-20
- [4] L.M. Petrila, F. Bucatariu, M. Mihai, C. Teodosiu, *Materials* 2021, 14(15), 1–30
- [5] F. Bucatariu, D. Schwarz, M. Zaharia, C. Steinbach, C.A. Ghiorghita, S. Schwarz, M. Mihai, *Colloids Surf. A Physicochem. Eng. Asp.* 2020, 603, 125211
- [6] C.A. Ghiorghita, F. Bucatariu, E.S. Dragan, *Cell. Chem. Technol.* 2018, 52, 663–672

Acknowledgment: This work was supported by a grant of the Ministry of Research, Innovation and Digitization, CNCS/CCCDI – UEFISCDI, project number PN-III-P2-2.1-PED-2019-1996, within PNCDI III

COMPOSITE MEMBRANES BASED ON SULFONATED POLY(ETHER ETHER KETONE) WITH POTENTIAL APPLICATION IN FUEL CELL

Laurențiu Baltag,^{1*} Petrisor Samoila¹, Adriana T. Marinoiu², Corneliu Cojocaru¹, Valeria Harabagiu¹

¹ *Petru Poni Institute of Macromolecular Chemistry, Laboratory of Inorganic Polymers, Iași, Romania*

² *National Research and Development Institute for Cryogenics and Isotopic Technologies—ICSI Râmnicu Vâlcea, Romania*

**baltag.laurentiu@icmpp.ro*

Global warming is one of the main issues humanity facing right now. The earth temperature started to grow since the pre-industrial period without any signs of stopping. One of the main challenges to combat global warming is the reduction of greenhouse gas emissions. To achieve this goal the entire energy system it is expected to be subjected to fundamental transformations [1]. The transportation sector will also have to change the internal combustion engine with a better alternative.

Proton-exchange membrane fuel cells (PEMFC), also known as polymer electrolyte membrane fuel cells, are a promising candidate for replacing internal combustion engine vehicles. The polymeric membrane is a key component that is responsible for proton conductivity, being directly related to the fuel cell efficiency and power. Unfortunately, the membrane prices are high and it is extremely challenging to develop membranes with desirable properties in terms of efficiency.

In this respect, considerable research efforts were done to find materials with similar or better properties, compared to commercially available PEM (Nafion), at lower cost. Sulfonated poly(ether ether ketone) (SPEEK) is one of the most promising material with potential for commercialization. SPEEK membranes have excellent chemical and thermal stability, good mechanical properties and electrical properties [2].

In this work we have used sulfonated poly(ether ether ketone) with a high degree of sulfonation (DS) and inorganic fillers, such as titanium oxide and cobalt ferrite, to develop membranes with appropriated characteristics to be used as PEM. The DS of the sulfonated polymer was determined by back titration method [3]. The membranes were prepared by casting process using SPEEK with 94% DS and 1:1 DMSO and ethanol solution as casting solvent. The as-obtained membranes were tested for their water-uptake properties, endurance in oxidative environment (Fenton reactive) and in acidic solution with pH 3 (H₂SO₄). Structural characterization of membranes was performed by FTIR. Likewise, the membrane mechanical properties (Figure 1), thermal properties and proton conductivity (Table 1) were investigated. This research proposes SPEEK-based composite membranes for applications in fuel cells.

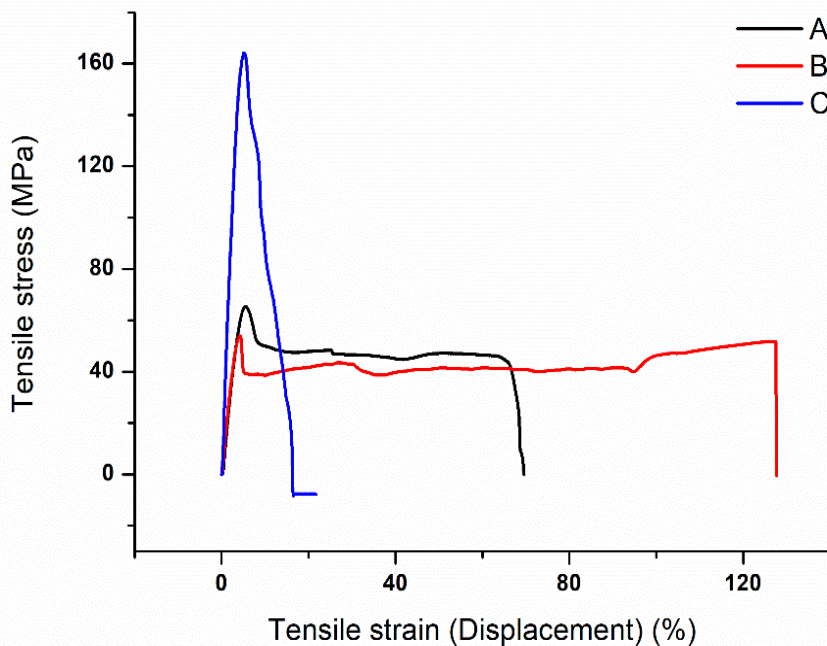


Figure 1. Mechanical properties of pristine SPEEK membrane (A), SPEEK membrane with TiO₂ (B) and with cobalt ferrite (C)

Table 1. SPEEK-based composite membranes proton conductivity

Membrane filler	Conductivity ($\Omega \text{ cm}^{-1}$)		
	40°C	60°C	80°C
-	0.201	0.244	0.338
Titanium dioxide (5%)	0.415	0.560	0.448
Cobalt ferrite (5%)	0.282	0.353	0.417

References

- [1] D. Möst, S. Schreiber, A. Herbst, M. Jakob, A. Martino, and W.-R. Poganietz, *The Future European Energy System: Renewable Energy, Flexibility Options And Technological Progress*, 1st ed. Springer, 2021.
- [2] C. M. Branco, A. El-kharouf, S. Du, *Materials for Polymer Electrolyte Membrane Fuel Cells (PEMFCs): Electrolyte Membrane, Gas Diffusion Layers, and Bipolar Plates*. Reference Module in Materials Science and Materials Engineering, Elsevier, 2017.
- [3] R. Y. M. Huang, P. Shao, C. M. Burns, and X. Feng, *Sulfonation of poly(ether ether ketone)(PEEK): Kinetic study and characterization*, *J. Appl. Polym. Sci.*, vol. 82, no. 11, pp. 2651–2660, 2001.

MONO- AND OLIGONUCLEAR COMPLEXES BASED ON SCHIFF BASE LIGAND

Ildiko Buta,^{1*} Sergiu Shova,² Sorina Ilies,¹ Florica Manea,³ Marius Andruh,⁴ Otilia Costisor¹

¹Coriolan Dragulescu Institute of Chemistry, Timisoara, Romania

²Petru Poni Institute of Macromolecular Chemistry, Iasi, Romania

³University Politehnica Timisoara, Faculty of Industrial Chemistry and Environmental Engineering, Timisoara, Romania

⁴University of Bucharest, Faculty of Chemistry, Inorganic Chemistry Laboratory, Bucharest, Romania

*ildiko_buta@acad-icht.tm.edu.ro

The chemistry of coordination compounds undergoes an important development once polynuclear compounds with special properties are obtained and recommended as materials with potential technological applications [1-5]. The formation of these compounds is controlled by the nature of the metal ions, the preorganizing ability of the ligands, as well as the experimental conditions [6]. Considering all of these aspects, compounds with desired properties and targeted application can be designed. As far as the ligands are concerned, Schiff bases are a class of organic compounds that are characterized by a high versatility due to the variety of their amino and carbonyl precursors [7].

Here, we present the obtaining of homo- and heteronuclear complexes, based on N,N'-bis[(3-methoxysalicylideneamino)-propyl]-piperazine (H₂L) Schiff-base ligand. The ligand has been crystallized in the H₂L·2DMSO form and its structure has been solved (figure 1).

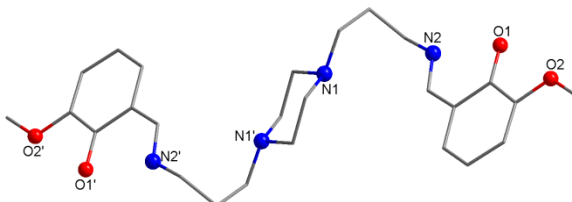


Figure 1. Molecular structure of H₂L [symmetry code: $i = -x, 1 - y, 1 - z$].

Using H₂L ligand, the following complexes have been synthesized: [CoL](ClO₄) (**1**), [Zn₂L(CH₃COO)₂]-2H₂O (**2**), [Cu₃L₂(NO₃)₂] (**3**) and [LaCu₆L₄(H₂O)₂(NO₃)₂](NO₃)₅·15H₂O (**4**). The **1** - **4** complexes were characterized by elemental analysis, X-ray crystallography, infrared and diffuse reflectance spectroscopy. X-ray diffraction shows that the H₂L and complexes **1** - **4** crystallize in $P2_1/c$ (H₂L and **1** - **3**) and $C2/c$ (**4**) space groups of monoclinic system. The Schiff base H₂L exhibits a stable *chair* conformation of the piperazine ring, while its coordination mode changes according to the nature of the metal ion and counterion, respectively, allowing the formation of mono- (**1**) and oligonuclear (**2** - **4**) complexes (figure 2).

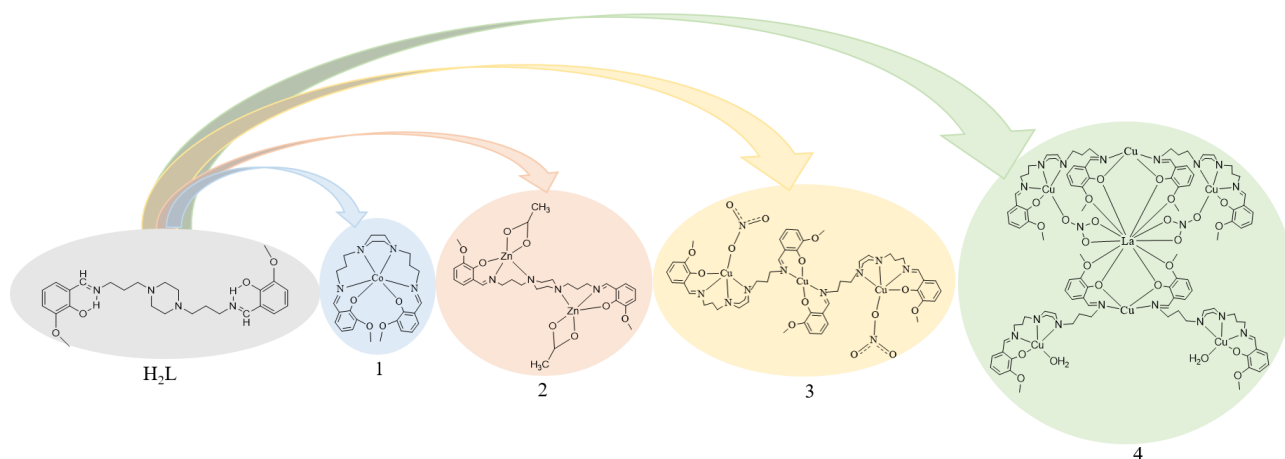


Figure 2. Schematic representation of H_2L and **1-4** complexes.

Compound **1** consists of a mononuclear complex cation, where the double-deprotonated ligand (L^{2-}) encapsulates the trivalent cobalt ion. In compound **2**, L^{2-} acts as a binucleating ligand through two N_2O sets of donor atoms disposed on each side of the piperazine ring. Compounds **3** and **4** contain trinuclear units where two ligands are coordinated to three Cu^{II} ions, with the N_3O donor set wrapped around the peripheral Cu^{II} . The remaining NO sets are bound to central Cu^{II} ion. In compound **4** two of this trinuclear moieties act as metalloligands towards the La^{III} ion, generating a heptanuclear compound. Electrochemical behavior of compounds **1** and **3** show a quasi-reversible behavior for **1** and irreversible behavior for **3**. Luminescent properties of compound **2** were investigated and the results were compared with that of the free H_2L ligand.

References

- [1] K.T. Mahmudov, A.V. Gurbanov, F.I. Guseinov, M. Fátima, C. Guedes da Silva, *Coord. Chem. Rev.* 2019, 387, 32-46.
- [2] J.M. Frost, K.L.M. Harriman, M. Murugesu, *Chem. Sci.* 2016, 7, 2470-2491.
- [3] K.D. Mjos, C. Orvig, *Chem. Rev.* 2014, 114, 4540-4563.
- [4] D.R. Slocombe, V.L. Kuznetsov, W. Grochala, R.J.P. Williams, P.P. Edwards, *Philos. Trans. A Math. Phys. Eng. Sci.* 2015, 373, 20140476.
- [5] K.K.-W. Lo, L.J. Charbonnière, *Eur. J. Inorg. Chem.* 2017, 5055-5057.
- [6] F.A.A. Paz, J. Klinowski, S.M.F. Vilela, J.P.C. Tomé, J.A.S. Cavaleiro, J. Rocha, *Chem. Soc. Rev.* 2012, 41, 1088-1110.
- [7] X. Liu, J.-R. Hamon, *Coord. Chem. Rev.* 2019, 389, 94-118.

Acknowledgment: We are thankful to the Romanian Academy, “Coriolan Dragulescu” Institute of Chemistry (Project 4.1.3) for financial support.

ELUCIDATION OF COMPLEX STRUCTURES THROUGH MASS SPECTROMETRY FRAGMENTATION STUDIES

Diana-Andreea Blaj,* Mihaela Balan-Porcarasu, Valeria Harabagiu, Cristian Peptu

Petru Poni Institute of Macromolecular Chemistry, Iasi, Romania

**blaj.diana@icmpp.ro*

Matrix-assisted laser desorption/ionization mass spectrometry (MALDI MS) represents a powerful technique for the characterization of complex chemical structures, allowing the identification of the monomer units and end chain groups, precise determination of the average molecular weights for polymer samples with narrow dispersity. Moreover, MALDI MS may be employed for witnessing the minute changes of the molecular weights during polymerization reactions, thus, expanding its use, as shown by previous studies concerning the ring-opening polymerization of lactide [1,2]. Herein, the solution ring-opening oligomerization (ROO) of D,L-lactide in the presence of β -cyclodextrin was considered as a case study to establish the reaction kinetics, for a better understanding of the chemical processes. Therefore, the reaction was performed using various parameters such as solvents, temperatures, molar ratios and, concentrations. Moreover, the reaction kinetics were established using both mass spectrometry and ^1H NMR spectroscopy to validate the obtained results. MALDI MS was successfully applied for monitoring the ring-opening of D,L-lactide in the presence of cyclodextrins with a particular emphasis on the structural elucidation of the secondary products resulting from side reactions. The main processes which may affect the structure of polylactides are related to transesterification. The reaction systems involving cyclodextrins are suitable for such studies since oligolactide chains grafted on cyclodextrins are spatially confined at relatively low distances from one another, thus favoring transesterification reactions. However, transesterifications are not the only possible side reaction as different solvents (N,N-dimethylformamide - DMF, N-methyl pyrrolidone – NMP) may interfere with the ROO process and lead to structural changes of the main product.

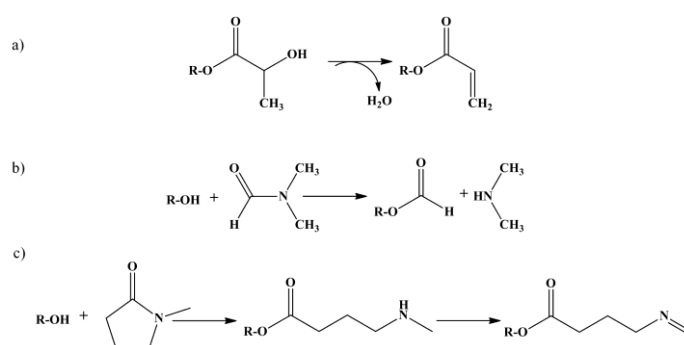


Figure 1. Degradation processes observed during the synthesis of CDLA: a) water elimination from oligolactides, b) cleavage of the DMF amide bond and c) cleavage of the NMP amide bond

Therefore, to have a deeper understanding of the chemical processes, MALDI MS was employed in the study of the reaction parameters. The solvent influence over the reaction kinetics was followed at different temperatures. Thus, the reactions performed in DMF and NMP solvents proceeded faster and led to higher values of the molecular weights in contrast with DMSO systems. These differences are consequences of an activation process in the ring-opening of lactide due to amines, acting as nucleophilic activators, resulting from the cleavage of the solvents' amide bonds, especially at higher temperatures [3,4], as depicted in **Figure 1**. The products resulting from degradation processes were identified in the MS spectra and structurally confirmed through MS/MS fragmentation experiments.

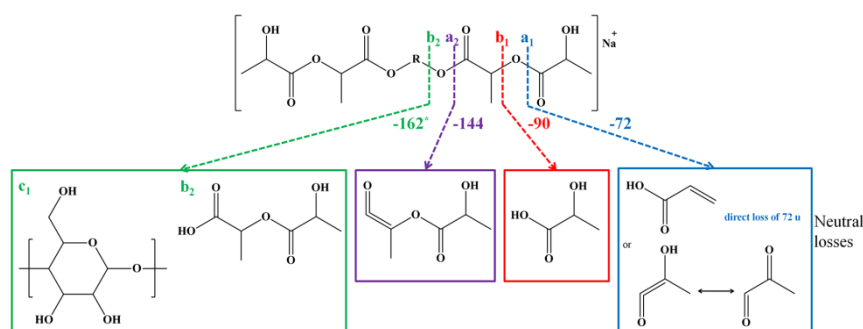


Figure 2. Fragmentation processes associated with main CDLA derivatives structures

The structures detected through direct MS measurements were confirmed using supplementary MS/MS fragmentation studies. Generally, cyclodextrin-oligolactide derivatives (CDLA) undergo two main types of fragmentations: oligosaccharide cleavages and oligolactide fragmentation at the level of ester bonds through 1-4 hydrogen rearrangements - cleavage of ester bond on the alkyl side and cleavages on the acyl side (1-3 hydrogen rearrangements or backbiting) – **Figure 2** [5-7]. The structural identification and confirmation of the secondary products could not be performed by NMR because of the low amounts relative to the total content of the CDLA samples. However, they were observed by MALDI MS and MS/MS fragmentation studies confirmed the structural assignment of the secondary products through the presence of specific neutral losses associated with the end chain groups of each series. Therefore, this study demonstrated the high value of mass spectrometry analysis in the structural characterization of complex polymerization systems.

References

- [1] O. Coulembier, J. De Winter, T. Josse, L. Mespouille, P. Gerbaux, P. Dubois, *Polym. Chem.* 2014, 5, 2103-2108.
- [2] D.A. Blaj, M. Balan-Porcarasu, B.A. Petre, V. Harabagiu, C. Peptu, *Polymer* 2021, 233, 124186.
- [3] J. Juillard, *Pure Appl. Chem.* 1977, 49, 885-892.
- [4] G. Lennon, S. Willox, R. Ramdas, S.J. Funston, M. Klun, R. Pieh, S. Fairlie, S. Dobbin, D.F. Cobice, *J. Anal. Methods Chem.* 2020, 8265054.
- [5] C. Peptu, M. Kowalczyk, O.F. van den Brink, J. Silberring, V. Harabagiu, B.C. Simionescu, *Pol. Sci. A Polym. Chem.* 2012, 50, 2421-2431.
- [6] S. Koster, M.C. Duursma, J.J. Boon, M.W.F. Nielen, C.G. de Koster, R.M.A.J. Heeren, *Mass Spectrom.* 2000, 35, 739-748.
- [7] J. De Winter, V. Lemaure, P. Marsal, O. Coulembier, J. Cornil, P. Dubois, P. Gerbaux, *J. Am. Soc. Mass Spectrom.* 2010, 21, 1159-1168.

Acknowledgment: This work was supported by the joint Romanian-Polish inter academic exchange project between „Petru Poni” Institute of Macromolecular Chemistry Iasi (Romanian Academy) and Center of Polymer and Carbon Materials Sciences of Zabrze (Polish Academy of Sciences) with the title “*PHA-based inclusion complexes with cyclodextrin – preparation and degradation study*”.

SYNTHESIS AND CHARACTERIZATION OF NOVEL POLYURETHANES BASED ON PIPERAZINE AND RENEWABLE CROSS-LINKERS

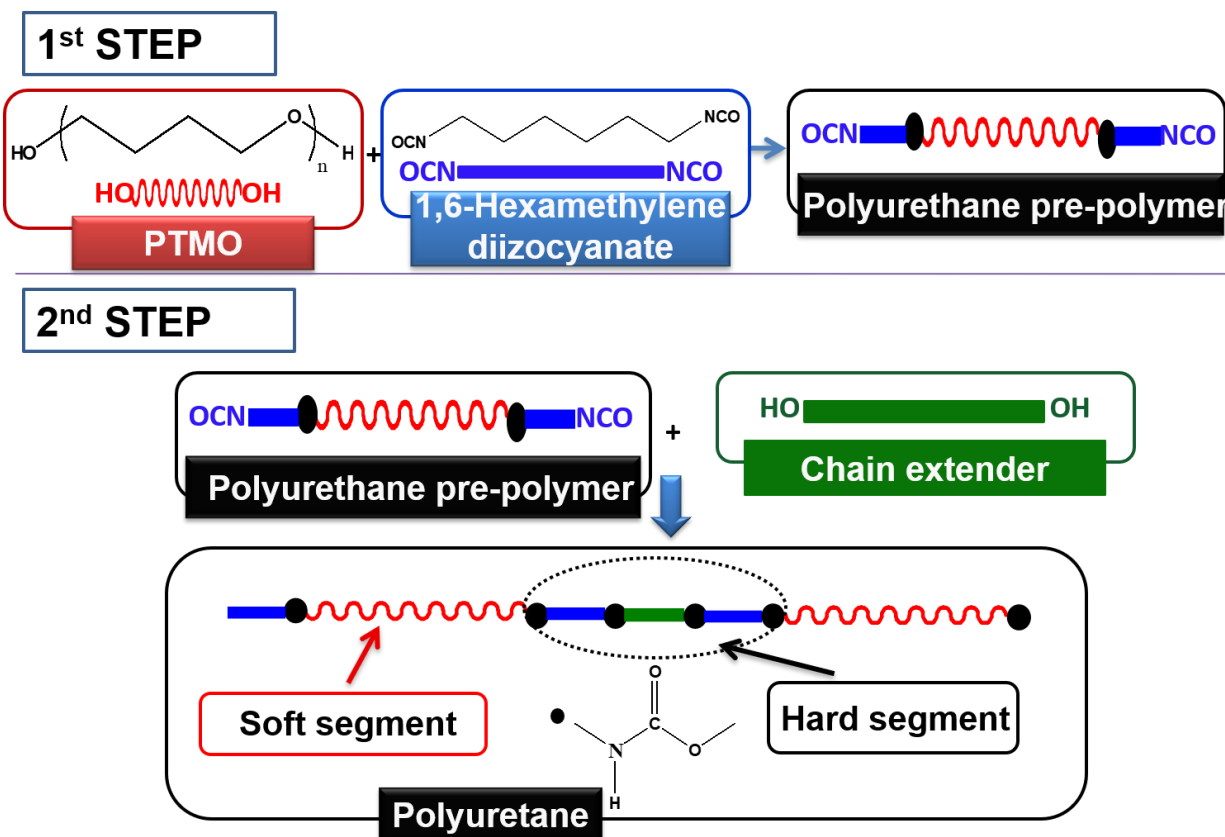
Violeta Otilia Potolinca,* Stefan Oprea

Petru Poni Institute of Macromolecular Chemistry, Iasi, Romania

**potolinca.otilia@icmpp.ro*

Segmented polyurethanes are a class of polymers of great importance with applications in a wide variety of fields such as medical materials, sealants, adhesives, automobiles, textile [1]. The specific properties of these materials derive from the incompatibility between hard and soft segments and the extent of phase separations. The structures of the hard segments have a great influence on the properties of the polyurethanes due to their physical crosslinking that acts as a polymer reinforcement matrix influencing in a significant way the performance of the obtained materials [2,3].

In order to combine the flexibility of the long aliphatic ether chains (poly (tetramethylene oxide) glycol) with a more rigid structure of the chain extender, we have included 1,4-piperazinediethanol (PDE) in the structure of the polyurethanes. PDE-based polyurethanes have remarkable properties, such as pH/temperature-sensitive, non-cytotoxic, biodegradable [4-6]. To increase the biodegradability character of the synthesized polyurethanes, we have chosen polyethylene glycol sorbitan monolaurate (Tween[®] 20) and sorbitan monolaurate (Span[®] 20) as cross-linkers. These have not been widely used in the synthesis of the polyurethanes as cross-linkers. The polyurethane synthesis procedure is illustrated in **Scheme 1**.



Scheme 1. The polyurethane synthesis diagram

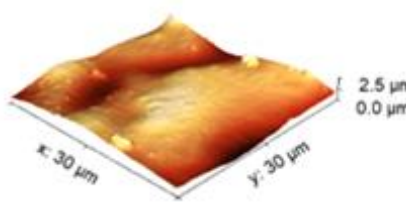
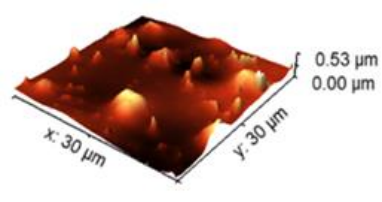
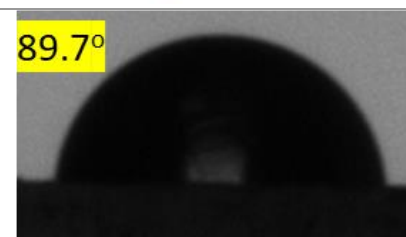
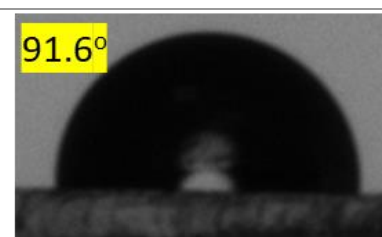
In addition, different ratios between hard and soft segment were considered in order to investigate the influence of the hard domains structure on the properties of the formed polyurethanes.

The morphological, thermal, mechanical and surface properties of the obtained PDE-based polyurethanes were thoroughly characterized using Fourier transform infrared (FTIR) spectra, differential scanning calorimetry (DSC), static contact angle measurements, atomic force microscopy (AFM) and mechanical tests. Also, thermal stability of the polyurethanes was analyzed by the weight loss measurement of the samples as the temperature increases.

FT-IR spectroscopy was used to confirm the chemical structure of the developed PDE-polyurethanes and also for the investigation of hydrogen bonding in polyurethane compounds. It was calculated the weight fraction of H-bonded urethane groups, the weight fraction of the hard segments in the soft phase of the polymers and the mixed phase weight fraction. It was found that the cross-linked polyurethanes were characterized by a higher degree of microphase mixing with respect to linear polyurethanes. Linear polyurethanes have good thermal stability with the 5% weight loss in the range 250-280 °C and cross-linked samples in the range 295-320 °C.

Table 1 presents several data on the properties of the synthesized polyurethanes. Phase mixing and phase separation of the hard and soft domains of the polyurethanes have a significant influence on the performance of the final polyurethane materials which will dictate the applicability range.

Table 1. Characteristics of the linear and cross-linked polyurethanes

Sample code	Linear polyurethane	Cross-linked polyurethane
Tensile strength [MPa]/Young Modulus [MPa]/Elongation at break (%)	38.38/26.09/1140	7.85/0.91/971
AFM images		
Water contact angle		

References

- [1] A. Das, P. Mahanwar, *Adv. Ind. Eng. Polym. Res.* 2020, 3, 93–101.
- [2] K. Kojio, S. Nozaki, A. Takahara, S. Yamasaki, *J. Polym. Res.* 2020, 27, 64–67.
- [3] S. Oprea, V.O. Potolinca, V. Oprea, *Eur. Polym. J.* 2021, 143, 110177.
- [3] W. Ye, L. Zhu, S. Xia, X. Zhang, *J. Polym. Eng.* 2018, 38, 371–379.
- [4] A. Wang, H. Gao, Y. Sun, Y.L. Sun, Y.W. Yang, G. Wu, Y. Wang, Y. Fan, J. Ma, *Int. J. Pharm.* 2013, 441, 30–39.
- [5] C. Ruan, Y. Wang, M. Zhang, Y. Luo, C. Fu, M. Huang, J. Sun, C. Hu, *Polym. Int.* 2012, 61, 524–530.

MULTI-STEP PROCEDURE LEADING TO A HETEROCYCLE CONTAINING DIMETHYLSILANE UNIT

**Madalin Damoc,* Alexandru Constantin Stoica, Diana Blaj, Ana-Maria Macsim,
Mihaela Dascalu, Maria Cazacu**

Petru Poni Institute of Macromolecular Chemistry, Iasi, Romania

**damoc.madalin@icmpp.ro*

Heterocycles containing silicon are still far away from being known enough. The number of such kind of structures remains limited, despite the fact that these compounds would be of great interest as photoelectric elements, for preparation of stable electrolytes or nanohybrid catalysts [1]. For the synthesis of heterocycles, the transition metals-catalyzed reactions are widely used. Thus, palladium-catalyzed cyclization reactions by carbonylation, carboxamidation and aldol condensation of active methylene were reported [2-4]. Herein, aiming in synthesis of platinum metal complexes, a new ligand containing dimethylsilane moiety has been developed by a two-step reaction, respectively Williamson and Schiff Base condensation, starting from bis(chloromethyl)dimethylsilane, 3,5-dichlorosalicylaldehyde and 2-aminophenol. By reacting the new compound with Pt(acac)₂, an uncommon cyclic structure, without metal, was unexpectedly obtained. The structures of the intermediate and final compounds were elucidated by elemental and spectral (FTIR, NMR, MALDI-MS) analyses, and X-ray diffraction (Figure 1).

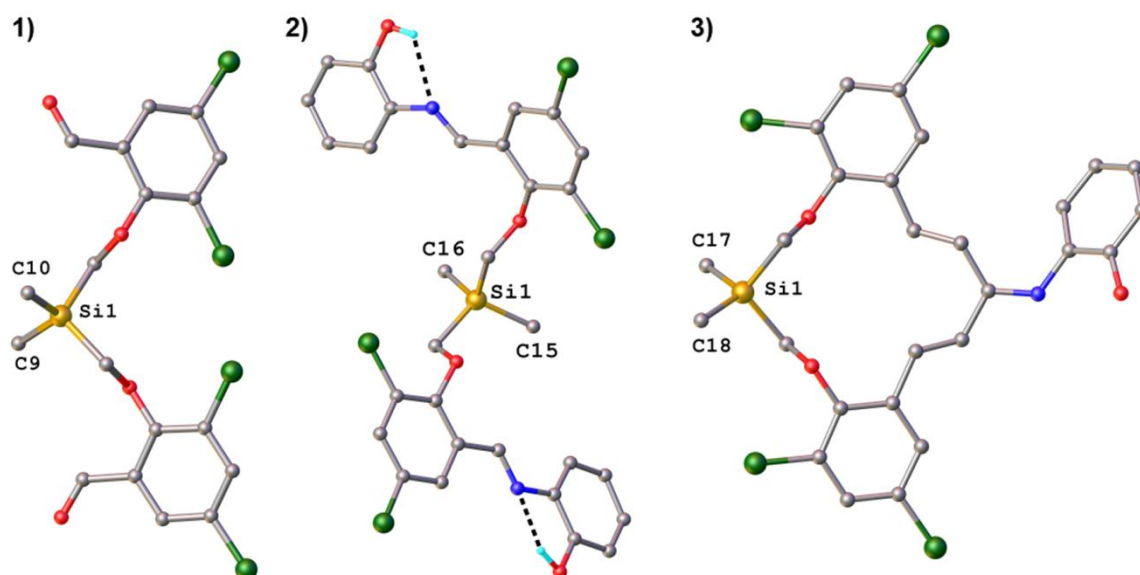


Figure 1. Structures determined by single crystal X-ray diffraction: product of Williamson condensation (1); product of imine condensation (2); product of cascade reaction (3)

As a consequence of unforeseen, a deep insight in the reaction mechanism and reaction conditions was required. 2D NMR or MALDI-MS studies reveal that the rearrangement processes and cascade reaction occur in three main steps, respectively imine cleavage, aldol condensation, and a new imine bond formation (Figure 2), all these being triggered by the platinum catalyst.

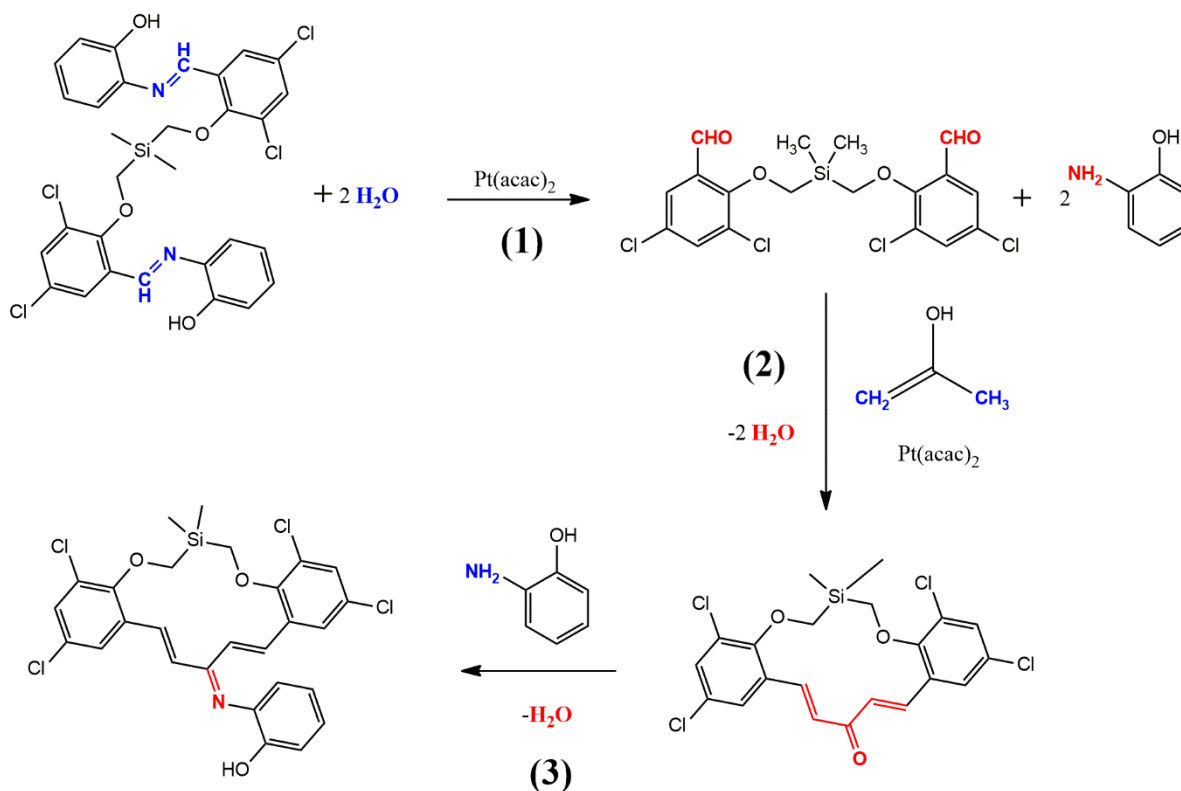


Figure 2. The proposed reaction mechanism of heterocycle **3** formation by cascade reaction

Studies have shown that in the complete reaction mixture, acetone in enol form is involved in the intermediate stage of aldol condensation. Without it, cyclization does not take place. Investigations on each of the reactants in the presence of the $\text{Pt}(\text{acac})_2$ complex have shown that dialdehyde **1** suffers fragmentation with the loss of the dimethylsilane fragment, while bis(imine) **2** predominates cyclization, in both reactions identifying the presence of 5,7-dichloro-2,3-dihydrobenzofuran-3-ol. The two reactions are concurrent. This novel route has many advantages, such as pretty good atom efficiency, catalyst recovery or the fact that it occurs at room temperature.

The underlying mechanism could be a real challenge in modeling new compounds involving a new C-C carbon bond by aldol condensation in the intermediate stage, but the remaining question is whether it will work in other systems.

References

- [1] N.O. Yarosh, L.V. Zhilitskaya, L.G. Shagun, I.A. Dorofeev, L.I. Larina, L.V. Klyba, *Russ. J. Org. Chem.* 2016, 8, 1223-1226.
- [2] G.Chouhan, H. Alper, *Org. Lett.* 2008, 21, 4987-4990.
- [3] C. Larksarp, H. Alper, *J. Org. Chem.* 1999, 64, 4152-4158.
- [4] F. Zeng, H. Alper, *Org. Lett.* 2010, 6, 1188-1191.

Acknowledgment: This work was supported by a grant of the Ministry of Research, Innovation and Digitization, CNCS/CCCDI – UEFISCDI, project number PN-III-P4-ID-PCE-2020-2000, within PNCDI III (Contract 207/2021, PerMONSi).

TRIAPINE ANALOGUES AND THEIR COPPER(II) COMPLEXES: SYNTHESIS, CHARACTERIZATION, SOLUTION BEHAVIOR, REDOX ACTIVITY, CYTOTOXICITY AND MR2 RNR INHIBITION

**Juliana Besleaga,^{1*} Iryna Stepanenko,¹ Tatsiana V. Petrasheuskaya,^{2,3} Denisa Darvasiova,⁴
Martin Breza,⁴ Marta Hammerstad,⁵ Małgorzata A. Marć,^{2,6} Alexander Roller,¹
Gabriella Spengler,^{6,3} Ana Popović-Bijelić,⁷ Eva A. Enyedy,^{2,3} Peter Rapta,³
Anatoly D. Shutalev,⁸ Vladimir B. Arion¹**

¹University of Vienna, Institute of Inorganic Chemistry, Vienna, Austria

²Department of Inorganic and Analytical Chemistry, Interdisciplinary Excellence Centre, University of Szeged, Szeged, Hungary

³MTA-SZTE Lendület Functional Metal Complexes Research Group, University of Szeged, Szeged, Hungary

⁴Institute of Physical Chemistry and Chemical Physics, Faculty of Chemical and Food Technology, Slovak University of Technology in Bratislava, Bratislava, Slovak Republic

⁵Section for Biochemistry and Molecular Biology, Department of Biosciences, University of Oslo, Oslo, Norway

⁶Department of Medical Microbiology and Immunobiology, University of Szeged, Szeged, Hungary

⁷Faculty of Physical Chemistry, University of Belgrade, Belgrade, Serbia

⁸N. D. Zelinsky Institute of Organic Chemistry, Russian Academy of Sciences, Moscow, Russian Federation
*besleagai96@univie.ac.at

Thiosemicarbazones (TSCs) are known as biologically active compounds with a broad spectrum of pharmacological properties, including anticancer activity.^{1,2} The cytotoxic properties may significantly augment by coordination to physiologically relevant metal ions, such as copper(II), which is as an essential trace element, redox-active, biocompatible and less toxic than non-endogenous heavy metals. One of the most well-known TSC is 3-aminopyridine-2-carboxaldehyde TSC (triapine), that was tested in more than 30 clinical phase I and II trials and currently is involved in a triapine-cisplatin-radiation combination therapy in a phase III trial.³ The iron containing ribonucleotide reductase (RNR) is considered as one of the main targets for triapine and related α -N-pyridinecarboxaldehyde TSCs.⁴ Due to the documented side effects (*e.g.*, methemoglobinemia) of triapine and its unfavorable pharmacokinetic profile (*e.g.*, short plasma half-life)⁵ development of novel TSCs with improved pharmaceutical properties and established mechanism of action is of high research interest.

In this work we report the synthesis of new triapine derivatives **HL¹–HL³**, which contain a potentially redox-active 4-aminophenolic unit, and of copper(II) complexes **1–3** (Chart 1). The crystal structures of TSCs **HL¹–HL³** and complexes **[Cu(L^{1–3})Cl]** were established by SC-XRD revealing the tridentate (N,N,S) coordination mode of the ligands. The presence of *E*- and *Z*-isomers with predominance of the first one in DMSO has been disclosed by 1D and 2D NMR spectroscopy. These data along with DFT calculations on model compound 2-formylpyridine TSC indicate that *Z/E* isomerization involves inversion at the aldimine nitrogen atom, rather than a tautomeric shift of the thioamide N2H proton to the pyridine nitrogen, followed by rotation around C–N1 bond as suggested previously.⁶ The relatively high Gibbs free energy barrier (~35.3 kcal/mol) for the *Z/E* conversion rules out the possibility of isomerization at room temperature, in agreement with time-dependent NMR data.

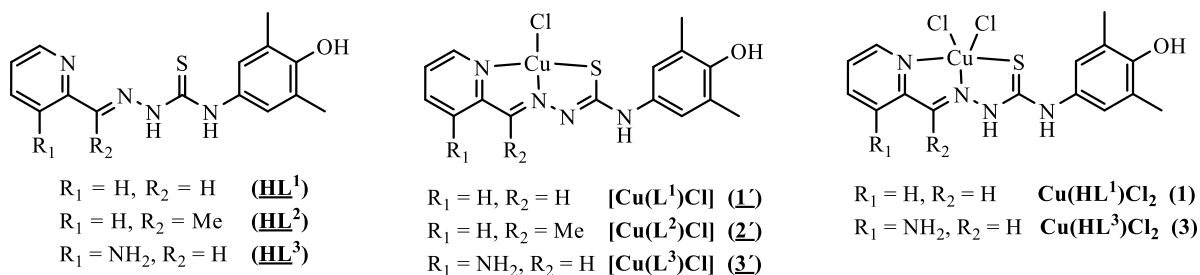


Chart 1. TSCs and their copper(II) complexes studied in this work. Underlined labels/numbers indicate compounds studied by single crystal X-ray diffraction (SC-XRD). The five-coordination of copper(II) in **1** and **3** has not been confirmed by X-ray crystallography.

Solution (equilibrium) studies revealed that the metal-free ligands are stable as **HL¹–HL³** at pH 7.4, while being air sensitive in the basic pH range. The monocationic complexes [Cu(L¹⁻³)]⁺ are the most abundant species in aqueous solutions at pH 7.4.

Electrochemical and spectroelectrochemical studies of **1**, **2'** and **3** confirmed their redox activity in both the cathodic and the anodic region of potentials. The one-electron reduction was identified as metal-centered by EPR spectroelectrochemistry. Electrochemical oxidation pointed out on the ligand centered oxidation, while chemical oxidation of **HL¹** and **HL²**, as well as **1** and **2'** afforded several two-electron and four-electron oxidation products, which were isolated and comprehensively characterized.

The anticancer activity of the obtained products was tested against two human cancer cell lines (doxorubicin-sensitive Colo205 and the multidrug resistant Colo320 human colonic adenocarcinoma) and normal human embryonal lung fibroblast cells (MRC-5) along with their mR2 RNR inhibiting ability. The metal-free ligands and several oxidized products showed no or only a moderate cytotoxicity against doxorubicin-sensitive Colo205 and the multidrug resistant Colo320 human colonic adenocarcinoma cell lines. Their copper(II) complexes revealed high cytotoxic potency when compared to that of the corresponding metal-free ligands. [Cu(L²)Cl] showed the highest cytotoxic activity with IC₅₀ values in the low micromolar concentration range, while Cu(HL³)Cl₂ has the highest selectivity for cancer cells over the normal fibroblast MRC-5 cells. In addition, **HL¹–HL³** and their copper(II) complexes were found to efficiently quench the tyrosyl radical in mR2 RNR in the presence of DTT as external reductant. The capacity of **HL¹** to destroy the tyrosyl radical is almost identical with that of triapine, which is by factor 1000 more potent R2 RNR inhibitor than hydroxyurea, a known clinical drug.⁷ Thus the copper(II) complexes reported herein deserve further investigation as potential anticancer drugs.

References

- [1] Matesanz, A.; Souza, P. *MRMC* **2009**, 9 (12), 1389–1396.
- [2] Garcia-Tojal, J.; Gil-Garcia, R.; Gomez-Saiz, P.; Ugalde, M. *CIC*, **2011**, 1 (2), 189–210.
- [3] Merlot, A. M.; Kalinowski, D. S.; Richardson, D. R. *Antioxidants & Redox Signaling*, **2013**, 18 (8), 973–1006.
- [4] Aye, Y.; Long, M. J. C.; Stubbe, J. *J. Biol. Chem.* **2012**, 287 (42), 35768–35778.
- [5] Nutting, C. M.; van Herpen, C. M. L.; Miah, et. At. *Annals of Oncology*, **2009**, 20 (7), 1275–1279.
- [6] Venkatachalam, T. K.; Pierens, G. K.; Reutens, D. C. *Synthesis, Magn. Reson. Chem.*, **2014**, 52 (3), 98–105.
- [7] Popović-Bijelić, A.; Kowol, C. R.; Lind, M. E. S.; Luo, J.; Himo, F.; Enyedy, É. A.; Arion, V. B.; Gräslund, A. *J. Inorg. Biochem.*, **2011**, 105 (11), 1422–1431.

ENHANCED PHOTODEGRADATION OF EVANS BLUE BY NOVEL SAMARIUM DOPED ZINC ALUMINIUM SPINEL FERRITES

Greco Ionela,* Samoila Petrisor, Corneliu Cojocaru, Petronela Pascariu, Valeria Harabagiu
Petru Poni Institute of Macromolecular Chemistry, Iasi, Romania
*greco.ionela@icmpp.ro

Water is the most vital among all natural resources and considered the most important for maintaining a healthy ecological balance. Economic development and environmental restoration guided by policies contributed to a profound impact on the relationship between ecosystem service supply and consumption in the past few decades. Due to human ignorance, a large number of water resources get contaminated daily and become unsuitable for drinking and other purpose. By promoting domains such as pharmaceuticals, chemicals, textiles, petrochemicals, cosmetics, there has been reported worrying amounts of organic pollutants (phenolic compounds, azo dyes, hormones, pesticides and traces of metal ions) in water sources, disrupting the aquatic ecosystems and the general human health [1]. These compounds are inefficiently removed by conventional wastewater treatments, negatively impacting us, due to their toxicity, carcinogenic and mutagenic properties [2].

Therefore, the scientific community has developed additional advanced treatment technologies. Among them the advanced oxidation processes (AOPs), that can convert organic pollutants into less harmful or even innocuous compounds. One of the most effective AOPs is photocatalysis, which is characterized as a suitable substitute for the mineralization of organic pollutants. The mechanism of photocatalysis is based on the photoexcitation of semiconductors by irradiation with energy equal or greater than the band gap of the semiconductors. Under this condition, highly reactive radicals ($\text{HO}\cdot$, $\text{O}_2\cdot^-$), are produced from photogenerated electrons and holes that are unselective and powerful oxidizing species (**Figure**).

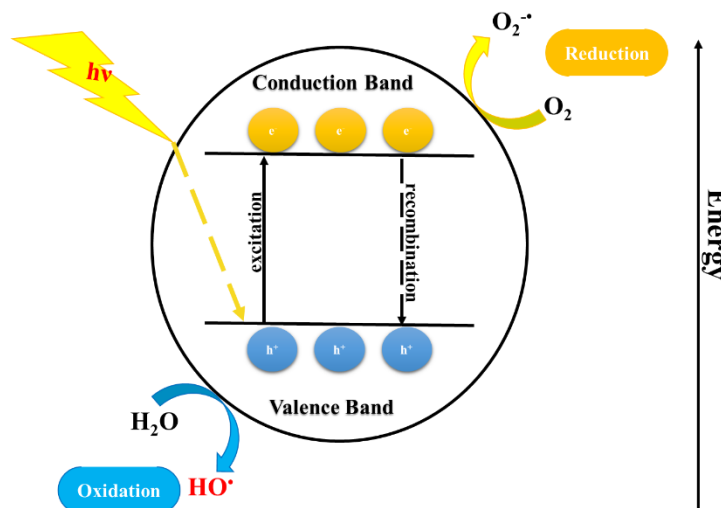


Figure 1. The mechanism of photocatalysis

The most common photocatalysts are known for certain limitations, such as low quantum efficiency, caused by the fast recombination of electrons and holes, and wide energy bandgap, which implies that they are activated only by the absorption of UV irradiation. Spinel ferrites have been in the lime light for their impressive performances in photodegradation due to its UV response, low cost, high sensitivity and their chemical and photochemical stability properties [3][4].

This study focuses on the synthesis and physico-chemical characterization of new samarium-doped spinel ferrites with photocatalytic properties, applied in Evans Blue dye photodegradation. The prepared ferrites, with the following general formula: $ZnAlFe_{1-x}Sm_xO_4$ ($x=0; 0.02; 0.04; 0.06; 0.08$), were doped with samarium in different ratios. The x-ray diffractograms show a decrease in the crystallite size once the dopant has been incorporated into the ferrite matrix (Table 1, Figure 2).

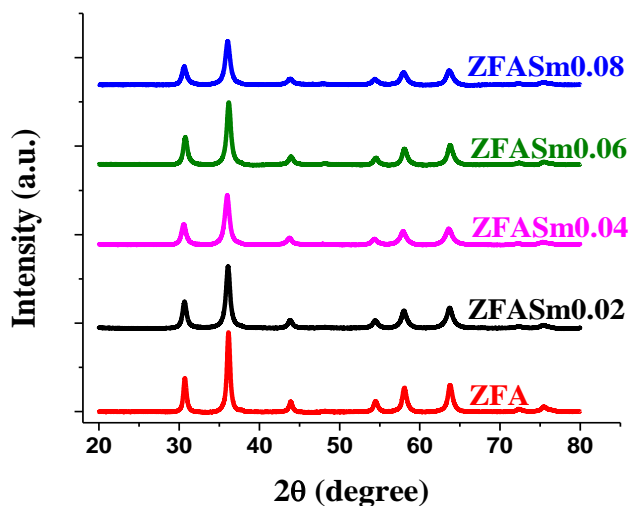


Figure 2. XRD patterns of doped and undoped zinc aluminium ferrites

Table 1. The dopant effect of samarium onto the crystallite size

Ferrite code	Dopant content (%)	Crystallite size (nm)
ZFA	-	14.65
ZFASm0.02	0.02	11.16
ZFASm0.04	0.04	9.91
ZFASm0.06	0.06	11.70
ZFASm0.08	0.08	10.02

In order to explain such behaviour, the characterization of materials was carried out by appropriate techniques, such as: Fourier transform infrared spectroscopy (FT-IR), X-ray diffraction (XRD), magnetic properties (VSM) and transmission electron microscopy (TEM).

References

- [1] G. Bal and A. Thakur, *Mater. Today Proc.*, 2021, 47, 19.
- [2] P. Samoila, C. Cojocaru, E. Mahu, M. Ignat, and V. Harabagiu, *J. Environ. Chem. Eng.*, 2021, 9(1), 104961.
- [3] P. Pascariu, M. Homocianu, C. Cojocaru, P. Samoila, A. Airinei, and M. Sucheai, *Appl. Surf. Sci.*, 2021, 476, p. 16–27.
- [4] A. R. Ribeiro, O. C. Nunes, M. F. R. Pereira, and A. M. T. Silva, 2014, 75, p. 33-51.

Acknowledgment: This work was supported by a grant of the Romanian Ministry of Research, Innovation and Digitization, CNCS/CCCDI–UEFISCDI, project number PN-III-P1-1.1-TE-2019-0594, within PNCDI III.

XANTHAN ACRYLATE/COBALT FERRITE MATERIAL FOR REMOVING DYES FROM WASTEWATERS

Irina Apostol,* Narcis Anghel, Iuliana Spiridon

Petru Poni Institute of Macromolecular Chemistry, Iasi, Romania;

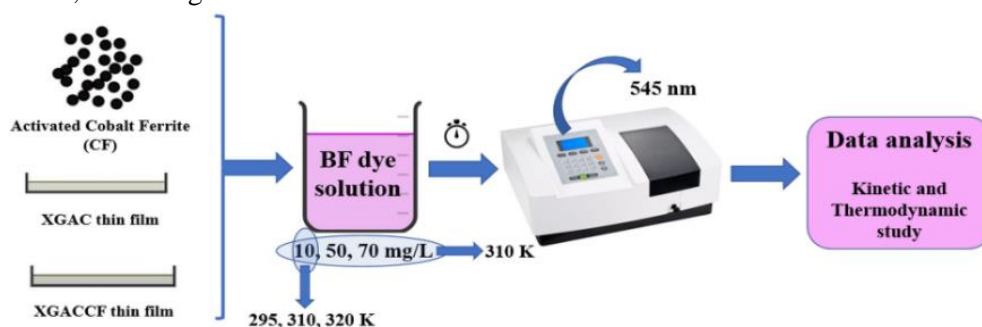
**apostol.irina@icmpp.ro*

Introduction

Pigments and dyes are used as chemicals in different industrial fields (foodstuffs, cosmetics, plastics or printing and leather industries). To reduce their negative effects on the human health, several materials with adsorptive properties has already been developed [1, 2]. Xanthan gum is a naturally occurring polysaccharide produced predominantly by *Xanthomonas Campestris*. In recent years, it has proved a significant potential in applications such as wastewater treatment or drug delivery, being a biodegradable and non-toxic compound [3]. Cobalt ferrite (CoFe_2O_4) is one of the most studied spinel materials due to its properties (magnetism, chemical stability or electrical insulation) and it can be embedded in different polymeric matrix [4]. In this study, xanthan/xanthan acrylate and cobalt ferrite were used to prepare materials with adsorptive properties.

Experimental

The CoFe_2O_4 powder (CF) was prepared by the co-precipitation method, using $\text{FeCl}_3 \cdot 6\text{H}_2\text{O}$ and $\text{CoCl}_2 \cdot 6\text{H}_2\text{O}$ as cation sources and castor oil as a dispersant agent. The resulted material was activated in a sodium citrate solution (concentration of 2%) to improve magnetic properties. Esterification of xanthan gum with acrylic acid was performed in order to increase hydrophobic character. Further, CoFe_2O_4 powder was embedded in acrylate xanthan (XGAC) matrix under ultrasonication, resulting a new material (XGACCF). The adsorption experiments have been performed to investigate the adsorption behavior of Basic Fuchsin (BF) dye from aqueous solutions, according to Scheme 1.



Scheme 1. Schematic illustration of adsorption experiments

Fourier transform infrared spectrometry (FT-IR) was used for the characterization of all materials. Kinetics of the adsorption experiments were studied by three models: pseudo-first order model, pseudo-second-order model and Elovich model, respectively. The adsorption of BF onto the adsorbents was thermodynamically evaluated by estimation of parameters such as Gibbs free energy (ΔG°), enthalpy (ΔH°) and entropy (ΔS°) derived from experimental data over the temperature range 295-320 K.

Results and discussions

FTIR spectra confirm the presence of the main bonds from studied materials (peaks at 580 cm^{-1} and 408 cm^{-1} can be related to the $\text{Co}^{2+}\text{-O}^{2-}$ or $\text{Fe}^{3+}\text{-O}^{2-}$ bonds from ferrite structure; absorption band of the carbonyl group at 1720 cm^{-1} confirms the introduction of new ester groups in the structure of xanthan). Kinetic parameters are

presented in Table 1. The determined R^2 values from pseudo-second-order kinetics ($R^2 > 0.9384$) of adsorbents are higher than those obtained from the pseudo-first-order kinetics ($R^2 > 0.7597$).

Furthermore, the amount of dye retained at equilibrium (q_e (cal)) obtained from the pseudo-second-order kinetic model is closer to the experimental q_e values.

This indicates that the chemisorption is relatively dominant for the BF adsorption and controls the process. It also can be observed that XGACCF presented the highest adsorption capacity.

Table 1. Kinetic parameters for adsorption of BF onto studied materials

Material	C_0 (mg/L)	q_e (exp) (mg/g)	Pseudo First Order			Pseudo Second Order			Elovich		
			q_e (cal) (mg/g)	$k_1 \times 10^{-5}$ (min ⁻¹)	R^2	q_e (cal) (mg/g)	$k_2 \times 10^{-5}$ (g/min×mg)	R^2	α (mg/g×min)	β (g/mg)	R^2
CF	10	6.33	5.59	5.62	0.97989	7.34	29.263	0.98841	0.674	0.398	0.97707
	50	10.02	8.62	4.42	0.98061	11.75	14.484	0.97076	0.415	0.494	0.95375
	70	11.49	11.86	4.541	0.97468	17.07	4.4518	0.95647	0.291	0.318	0.95359
XGAC	10	9.56	6.90	6.337	0.93748	10.24	42.354	0.99609	0.601	2.100	0.99465
	50	16.56	16.98	9.47	0.9877	19.11	15.696	0.99907	0.247	1.253	0.97912
	70	24.93	19.61	8.645	0.98755	27.16	17.675	0.99977	0.207	4.278	0.97782
XGACCF	10	7.96	11.11	10.5	0.91642	9.92	18.991	0.99513	0.454	0.398	0.9897
	50	48.77	53.90	6.05	0.90084	95.40	8.76	0.92815	0.064	1.459	0.96265
	70	63.35	122.2	10.28	0.75978	95.42	8.76	0.93841	0.047	1.743	0.9719

The effect of temperature on the adsorption capacity of the prepared materials was investigated at 295, 310 and 320 K, using a dye solution of 10 mg/L concentration. The thermodynamic parameters are presented in Table 2. It was evidenced that the BF retention is an exothermic process.

Table 2. Thermodynamic parameters for the removal of BF onto studied materials

Sample	Dye (10 mg/L)	ΔH° (kJ/mol)	ΔS° (kJ/mol×K)	ΔG° (kJ/mol)		
				295 K	310 K	320 K
CF	BF	-150060	-479.46	-4782.6	51.54	4416.39
XGAC	BF	-40655.5	-121.8	-3441	-3005.2	-1130.7
XGACCF	BF	-27103	-75.45	-4348.5	-3020.6	-2982.4

Conclusions

Xanthan acrylate/cobalt ferrite material was obtained and its adsorptive properties were studied. Batch adsorption experiments showed that the BF adsorption process followed pseudo-second-order kinetic model, the retention process being exothermic. The adsorption capacity of BF dye onto XGACCF as compared to that of XGAC was twice more efficient due to the CF addition.

References

- [1] F.M. Alzahrani, N.S. Alsaiani, K.M. Katubi, A. Amari, F.B. Rebah, M.A. Tahoona, *Polymers* 2021, 13, 1742.
- [2] L.I. Abd Ali, H.K. Ismail, H.F. Alesary, H.Y. Aboul-Enein, *Int J Environ Sci Technol* 2021, 18, 2031–2050.
- [3] M.H. Abu Elella, E.S. Goda, M.A. Gab-Allah, S.E. Hong, B. Pandit, S. Lee, H. Gamal, A. ur Rehman, K.R. Yoon, *J. Environ. Chem. Eng.* 2021, 9, 104702.
- [4] R. Jayalakshmi, J. Jeyanthi, *J. Environ. Chem. Eng.* 2021, 9, 104924.

IN SILICO STUDIES OF A NOVEL AMPHIPHILIC GRAFT CONJUGATED POLYMER FOR BIOMEDICAL APPLICATIONS

Petru Țirnovan,^{1,*} Francesca Mocci,^{1,2} Tudor Vasiliu,¹

Luminița Cianga,¹ Ioan Cianga,¹ Mariana Pinteală,¹ Aatto Laaksonen^{1,3}

¹*Centre of Advanced Research in Bionanoconjugates and Biopolymers, Petru Poni Institute of Macromolecular Chemistry, Iasi, Romania*

²*Department of Chemical and Geological Sciences, University of Cagliari, Monserrato, Italy*

³*Division of Physical Chemistry, Department of Materials and Environmental Chemistry, Arrhenius Laboratory, Stockholm University, Stockholm, Sweden*

*tirnovan.petru@icmpp.ro

Amphiphilic structures are very interesting and important constructions due to their capability to generate complexity at the nanoscale level, inducing in this way novel features to materials [1], many of them with applicability in the biomedical field. More specifically, amphiphilic polymers are particularly attractive because of their inherent self-assembling tendency; thus, they play an important role in biomedical applications including diagnosis, therapy and tissue engineering [2]. On the other hand, graft-shaped polymers are considered the most important polymer structure among the whole class of branched architectures, especially because a plethora of properties can be manipulated through side chains stimuli sensitivity, nature, length and grafting density. In particular, in the last decade it has been shown that amphiphilic grafted π -conjugated polymers (CPs) can be optimal candidates for diagnosis, drug delivery and combinatorial therapies [3], for biosensors [4] or for tissue engineering [5].

The inherent rod-like stiffness of the conjugated main chain, besides its fluorescence, electrical properties and π - π interaction capability as well as the structural stiff asymmetry between the rod-like main chain and flexible coil-like side chains determine the grafted CPs' uniqueness. If the heterografted copolymer PTh-*g*-(PEG-*r*-PCL) is considered, it contains a π -conjugated polythiophene (PTh) main chain and polyethylene glycol (PEG) and poly- ϵ -caprolactone (PCL) as the side chains randomly distributed along the main chain [4]. Because of their amphiphilic character and their complex topology, PTh-*g*-(PEG-*r*-PCL) copolymers may be used as building blocks for a variety of multidomain nanoscale structures that emerge as a result of hierarchical intra- and intermolecular self-organization in selected solvents. When the solvent is not good for the main chain but is good for the grafts, the main chain is collapsing, resulting in intramolecular micelles with different morphologies which are stabilized against aggregation due to repulsive interactions of the grafts. When the solvent is good for the main chain and poor solvent for the grafts then changes in morphology can occur [6].

The aim of the present study is to analyze the morphological changes in PTh-*g*-(PEG-*r*-PCL) amphiphilic graft copolymer by using molecular dynamics simulations in different solvents. We introduce the computational model and method. We describe the building and preparation of the system for simulations. It employs the usage of AmberTools suite for residue definition, GAFF2 force field for parameter calculation and RESP charge derivation for calculating the charges of atoms. The simulations were done using AMBER 18 [7]. The procedure is described as follows.

Fragments were required for residues definition, for which force field parameters were calculated. After residues were defined, parameters were calculated, involving bonds, angles and dihedrals, along with atomic charges. The complete structure of the molecule (molecule A from **Figure 1**) was obtained after loading every fragment in xleap/tleap module.

Implicit solvent models despite being much faster than explicit models do not represent the proper behavior of this compound because the "physical" presence of solvent molecules in the system has a very important role

in the supramolecular structure. This leads to a very similar behaviour in all the solvents used. On the other hand, explicit solvent models although requiring a larger calculation power, are considerably better at representing the experimental behaviour. In this situation, the structure is more dynamic, with the side chains continuously transitioning back and forth from a collapsed state to elongated as illustrated below:

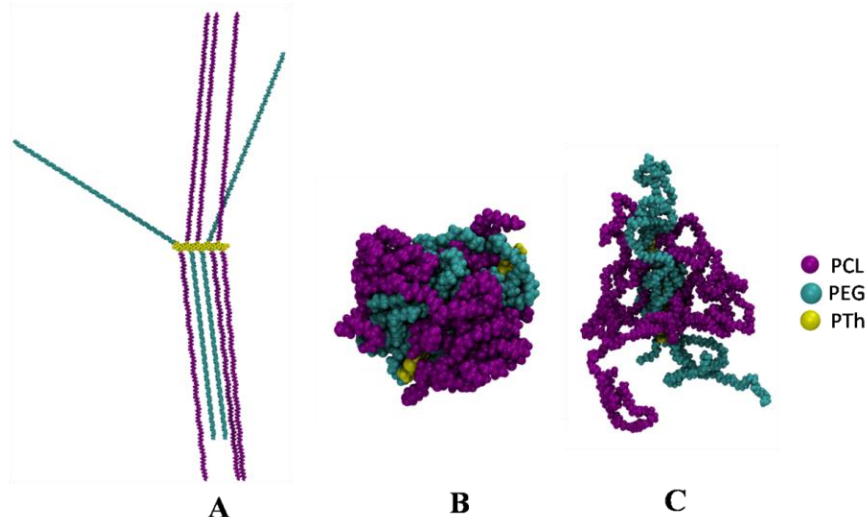


Figure 1. Depictions of the supramolecular structure of the copolymer:
A) starting structure, B) implicit solvent, C) explicit solvent

References

- [1] P. Calandra, D. Caschera, V. Turco Liveri, and D. Lombardo, “How self-assembly of amphiphilic molecules can generate complexity in the nanoscale,” *Colloids Surfaces A Physicochem. Eng. Asp.*, vol. 484, pp. 164–183, 2015.
- [2] F. Perin, A. Motta, and D. Maniglio, “Amphiphilic copolymers in biomedical applications: Synthesis routes and property control,” *Mater. Sci. Eng. C*, vol. 123, p. 111952, 2021.
- [3] C. Xie, W. Zhou, Z. Zeng, Q. Fan, and K. Pu, “Grafted semiconducting polymer amphiphiles for multimodal optical imaging and combination phototherapy,” *Chem. Sci.*, vol. 11, no. 39, pp. 10553–10570, 2020.
- [4] B. G. Molina, L. Cianga, A.-D. Bendrea, I. Cianga, C. Alemán, and E. Armelin, “An amphiphilic, heterografted polythiophene copolymer containing biocompatible/biodegradable side chains for use as an (electro)active surface in biomedical applications,” *Polym. Chem.*, vol. 10, no. 36, pp. 5010–5022, 2019.
- [5] A. D. Bendrea *et al.*, “Polythiophene-g-poly(ethylene glycol) graft copolymers for electroactive scaffolds,” *J. Mater. Chem. B*, vol. 1, no. 33, pp. 4135–4145, 2013.
- [6] K. H. Shen, M. Fan, and L. M. Hall, “Molecular Dynamics Simulations of Ion-Containing Polymers Using Generic Coarse-Grained Models,” *Macromolecules*, vol. 54, no. 5, pp. 2031–2052, Mar. 2021.
- [7] T. A. D. D.A. Case, I.Y. Ben-Shalom, S.R. Brozell, D.S. Cerutti, T.E. Cheatham, III, V.W.D. Cruzeiro *et al.*, “AMBER 2018,” vol. University. 2018.

Acknowledgment: This work is supported from the PN-III-P4-ID-PCCF-2016-0050 grant, funded by the Ministry of Research and Innovation, CNCS/CCCDI–UEFISCDI, within the PNCDI III program.

ZWITTERIONIC POROUS MICROPARTICLES - ADVANCED MATERIALS AS POTENTIAL DRUG DELIVERY SYSTEMS

Marin-Aurel Trofin*, Stefania Racovita, Silvia Vasiliu, Ana-Lavinia Vasiliu, Marcela Mihai

Petru Poni Institute of Macromolecular Chemistry, Iasi, Romania

*marin.trofin@icmpp.ro

Zwitterionic microparticles with controllable structures and advanced functions allow enhancement of adsorption processes to achieve improved performances for drug delivery applications due to their good biocompatibility, non-toxicity, low immunogenicity and antifouling activity [1-3]. Thus, the purpose of this study was to obtain zwitterionic porous microparticles with potential application in drug delivery. The preparation of zwitterionic porous microparticles took place in two steps (Figure 1). First step consists in the synthesis of porous microparticles by suspension polymerization using glycidyl methacrylate (GMA), N-vinyl imidazole (NVI) and four types of crosslinking agents, such as: ethyleneglycol dimethacrylate (EGDMA), diethyleneglycol dimethacrylate (DEGDMA), triethyleneglycol dimethacrylate (TEGDMA) and divinyl benzene (DVB). The influence of different reaction parameters (monomer ratio, types of crosslinking agents, types of diluents, crosslinking degree) on the reaction yield and swelling capacity in different solvents was studied in order to find the optimal conditions for the synthesis. Microparticles with the following characteristics were chosen for further transformation: monomer ratio GMA:NVI:TEGDMA = 40:30:30 (mol:mol) and porogenic agent = toluene. The second step was the synthesis of zwitterionic porous microparticles by polymer-analogous reactions in the presence of betainization agent: sodium monochloroacetate.

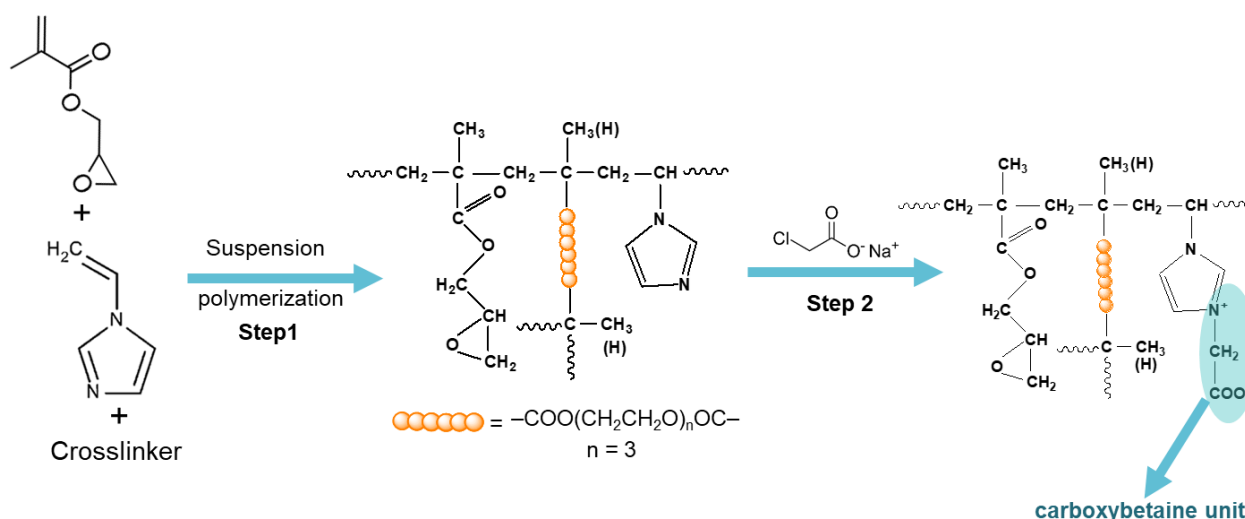


Figure 1. The synthesis of zwitterionic microparticles

The synthesized zwitterionic porous microparticles were characterized by FTIR spectroscopy, elemental analysis, particle size distribution and SEM analysis (Figure 2). After betainization reaction with sodium monochloroacetate the spherical shape of the microparticles is preserved but an increase of the pore size is observed at the surface of microparticles.

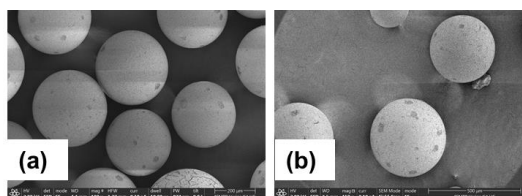


Figure 2. SEM images of porous microparticles before (a) and after betainization reaction (b).

The tetracycline loading into zwitterionic porous microparticles was also followed (Figure 3, A). The concentrations of drug in the supernatant solution before and after adsorption were determined using UV-VIS spectrophotometry based on a calibration curve. The maximum tetracycline loading capacities onto porous and zwitterionic porous microparticles were: 87 mg/g and 135 mg/g, respectively. To elucidate the drug transport mechanism involved in the release process of tetracycline from microparticles (Figure 3, B), various models were applied: Higuchi, Korsmeyer-Peppas and Baker-Lonsdale models.

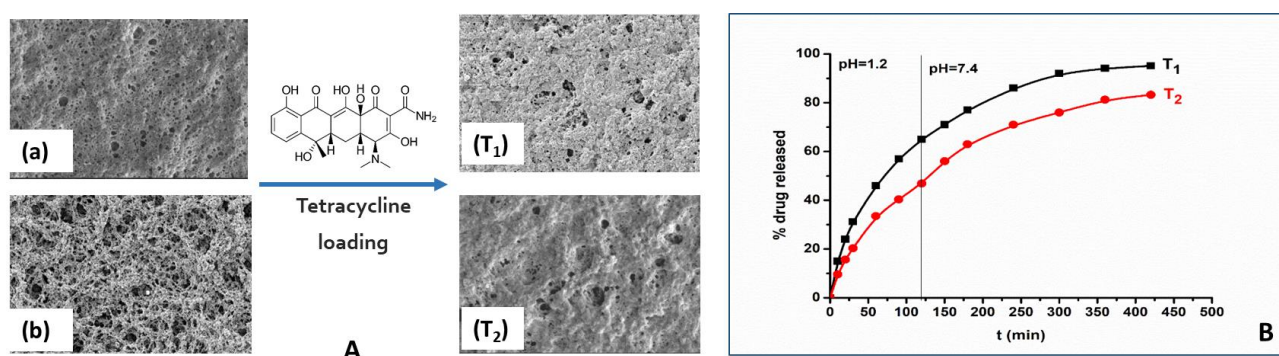


Figure 3. A. SEM images of porous microparticles before (a) and after (T₁) tetracycline loading and zwitterionic porous microparticles before (b) and after (T₂) tetracycline loading B. Drug release profile under simulated gastro-intestinal tract conditions.

Compared to porous microparticles where the drug is adsorbed only in pores, in the case of zwitterionic microparticles the tetracycline can interact with functional groups belonging to the crosslinked network chains through ionic and physical interactions. The release of drug takes place gradually by the dissociation of ionic interactions followed by the diffusion of drug through pores.

Thus, tetracycline can be loaded on the zwitterionic beads due to both physical and chemical interactions. Korsmeyer-Peppas diffusion coefficient is approx. 0.6 suggesting a non-Fickian transport mechanism. Therefore, zwitterionic porous microparticles can be used as drug delivery systems.

References

- [1] W.-Y. Liu, W. Wang, X.-J. Ju, Z. Liu, R. Xie, L.-Y. Chu, *Chem. Eng. Sci.* 2021, 231, 116242.
- [2] B. Wang, S. Wang, Q. Zhang, Y. Deng, X. Li, L. Peng, X. Zuo, M. Piao, X. Kuang, *Acta Biomater.* 2019, 96, 55–67.
- [3] S. Racovita, M.-A. Trofin, D. F. Loghin, M.-M. Zaharia, F. Bucatariu, M. Mihai, S. Vasiliu, *Int. J. Mol. Sci.* 2021, 22, 9321.

Acknowledgement

This work was supported by a grant of the Ministry of Research, Innovation and Digitization, CNCS/CCCDI – UEFISCDI, project number PN-III-P4-ID-PCE-2020-1541, within PNCDI III.

pH/TEMPERATURE-SENSITIVE INTERPENETRATING POLYMERIC HYDROGEL

Bogdan Cosman*, Sanda Bucatariu, Marieta Constantin, Gheorghe Fundueanu

Petru Poni Institute of Macromolecular Chemistry, Iasi, Romania

**E-mail: cosman.bogdan@icmpp.ro*

Introduction

The field of sensitive hydrogels has expanded rapidly in the last years, leading to many advances in designing and developing of multi-functional systems [1]. Among these, drug delivery systems (DDS) based on hydrogels had become a major area of research interest and many products have been developed [2]. One of the most commonly investigated temperature-sensitive hydrogel is based on poly(N-isopropylacrylamide) (PNIPAM) copolymers. This hydrogel exhibits a sharp temperature-dependent volume change close to the human body temperature. However, responsiveness to more than one stimulus can lead to a better control over the release of the drugs at the target site [3]. Despite their multiple benefits, single network hydrogels have yet weak mechanical properties and slow response at swelling, limiting their applications. By using the interpenetrating polymer network (IPN) strategy, many researchers have prepared IPN materials based on PNIPAM to improve the physico-chemical and mechanical properties, as well as drug loading/release capacity [4-6].

In this study, a thermosensitive hydrogel based poly(N-isopropylacrylamide-co-hydroxyethylacrylamide) (PNH) was interpenetrated with poly(methyl vinyl ether-co-maleic acid) (P) copolymer, aiming to synthesize a conventional hydrogel (CTH) that preserve thermosensitive properties as well as to reinforce its mechanical stability. Moreover, P was introduced to confer pH sensitivity to the hydrogel as well as for pharmaceutical and medical purposes due to its biocompatibility and low toxicity [7]. The morphology of IPN hydrogels as well as the main characteristics were investigated by Scanning Electron Microscopy (SEM), FTIR spectroscopy and Texture Analyzer (TA).

Experimental

CTH was obtained by radical copolymerization of N-isopropylacrylamide (N) and hydroxyethylacrylamide (H) in aqueous solution in the presence of N,N'-methylenebisacrylamide (B) at different molar ratio relative to the total moles of comonomers (0.4%; 0.6%; 0.8%). The obtained samples were noted **PNH_x**, where x means the molar percent of B vs comonomers. The N:H molar ratio of 10:2 was used, this value being already established [3] to be optimal for obtaining of a PNH linear copolymer with a lower critical solution temperature (LCST) value close to the human body temperature. In order to obtain the IPN hydrogels, the CTH samples were immersed for 3 days in P aqueous solutions of different concentrations (2 and 5%), until they reached the swelling equilibrium. Then, the swelled samples were lyophilized and then placed in an oven for 24 h, at 80 °C. The obtained samples were noted **IPN_x-P_y** where x means the molar percent of B vs comonomers and y the concentration of P solution.

Results and discussion

The IPN hydrogels were obtained by swelling the PNH hydrogels in P solution. Then, they were lyophilized and thermal treated at 80 °C for 24 h. The IPN hydrogels were successfully prepared with an yield of ~ 80%, with variable amounts of P gravimetrically determined. The proposed cross-linking mechanism, schematic representation of IPN synthesis and SEM images are given in Figure 1. The results from SEM and FTIR spectroscopy indicated that the second network was formed in the IPN hydrogels. Moreover, the IPN hydrogels with the highest content of P displayed a significantly improved mechanical properties than the rest of the

hydrogels.

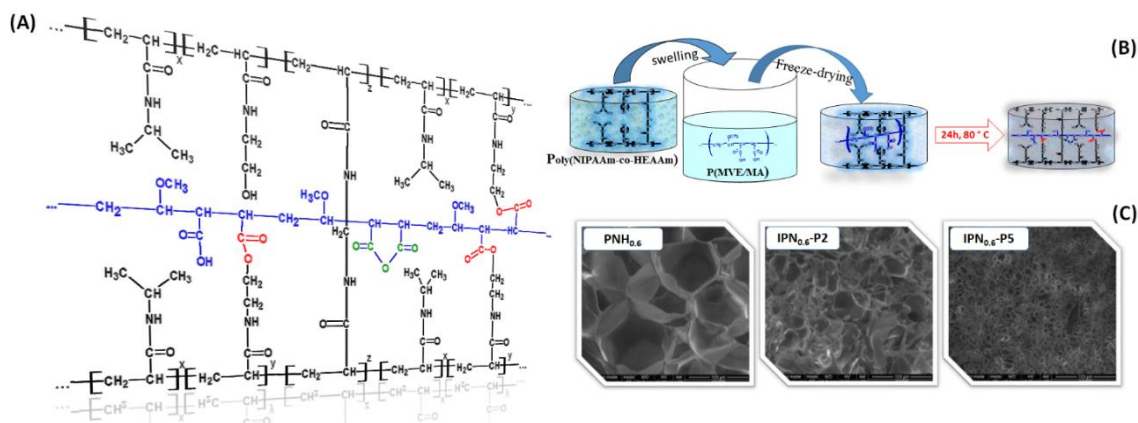


Figure 1. (A) Proposed cross-linking mechanism between PNH and P; (B) Schematic representation of IPN hydrogels synthesis; (C) SEM images of conventional and IPN hydrogels

The resulted data (related to the swelling behavior of the both CTH and IPN hydrogels at different temperatures and buffer solutions of different pH), demonstrated the IPN preserves the thermosensitive properties and, in addition, presents also the pH sensitivity. Thus, the swelling kinetics were strongly dependent on temperature (25 °C and 37 °C) and pH (7.4 and 1.2) conditions. *In vitro* loading/release studies of propranolol (Pp), used as a model drugs, into/from IPN indicated that the P component causes an enhanced loading for the ionized IPN and a reduction in the release rate in acidic conditions. *In vitro* experiments showed a sustained release of the propranolol from the IPN in an acidic medium, at 37 °C.

Conclusions

A new thermo- and pH-sensitive IPN hydrogel as a potential DDS, was obtained. SEM observations showed a decreasing in the pore size with increasing of P amount in the IPN hydrogels. Moreover, the P content in IPN was found to dictate the swelling/deswelling kinetic behavior as well as the release profile of the entrapped drug. Compared with the fast release rate from CTH, the release kinetics of Pp from IPN hydrogels exhibit a delayed release pattern in acidic medium. The new IPN hydrogels showed a promising performance for the controlled release of drugs.

References

- [1] A. Bratek-Skicki, *Appl. Surf. Sci. Adv.* 2021, 4, 100068.
- [2] S. Brahma, C. Boztepe, A. Kunkul, M. Yuceer, *Mater. Sci. Eng. C* 2017, 75, 425–432.
- [3] G. Fundueanu, M. Constantin, I. Asmarandei, S. Bucatariu et al., *Eur. J. Pharm. Biopharm.* 2013, 85, 614–623.
- [4] Z. Qin, R. Zhang, Y. Xu a, Y. Cao, L. Xiao, *JCIS Open I* 2021, 100002.
- [5] J.T. Zhang, R. Bhat, K. D. Jandt, *Acta Biomater.* 2009, 5, 488–497.
- [6] E.S. Dragan, *Pure Appl. Chem.* 2014, 86, 1707–1721.
- [7] A.V. Torres-Figueroa, C.J. Pérez-Martínez, J.C. Encinas, et al, *Pharmaceutics* 2021, 13, 1284.

Acknowledgment: This work was supported by a grant of Ministry of Research and Innovation, CNCS - UEFISCDI, project number PN-III-P4-ID-PCCF-2016-0050, within PNCDI III.

COPPER TETRANUCLEAR COMPLEX BEARING SILANOL FUNCTIONAL GROUPS

Alexandru-Constantin Stoica*, Madalin Damoc, Mihaela Dascalu, Maria Cazacu

*Petru Poni Institute of Macromolecular Chemistry, Department of Inorganic Polymers,
Iasi, Romania*

**stoica.alexandru@icmpp.ro*

Although more than 150 years have passed since their discovery, Schiff's bases still play an important role in the development of inorganic chemistry, being among the most common ligands for metals with which it forms complexes with different architectures. This is due to simple and easy procedures of synthesis and almost limitless possibilities to combine reagents (carbonyl compounds, amines and metals). Thus the structure and properties can be fine-tuned according to the requirements of different fields of applications [1]. Some of the most commonly used Schiff base ligands are the salen-type resulting from the condensation of a diamine with two equivalents of salicylic aldehyde or substituted derivatives thereof. These have four coordinating sites (two covalent and two covalent-coordinative bonds in a planar array) and, when coordinated to an octahedral metal center, leave two axial sites open for ancillary ligands [2]. If the initial attention was focused on the N,N'-ethylenebis(salicylaldimine), the product range expanded rapidly with extra functional group derivative, side chains or longer spacers, for example more methylene [3] or ethylene glycol groups [4]. In the last decade, we have developed a series of such ligands based on a diamine with tetramethyldisiloxane spacer, 1,3-bis(3-aminoropyl)tetramethyldisiloxane, and different aldehydes and complexation of different metal ions.

Here, our idea was to use another rare diamine, namely 1,3-bis(2-aminoethylaminomethyl)-tetramethyldisiloxanes (AEAMTMDS) prepared at the laboratory level in 2012 for use as curing agent for bisphenol A epoxy resin [5]. The use of this amine is also reported as liquid carbon dioxide absorbents [6]. AEAMTMDS was treated with 3-formylsalicylic acid (3-FSA), in solution, in a slightly acidic medium, and immediately, without product isolation, with the copper salt to obtain the metal complex **1** in a one-pot procedure.

The crystalline reaction product, resulted in quite high yield, was analyzed from a structural point proving to be a dinuclear complex with a methylaminoethylsilanol arm (**Figure 1a**). It is assumed that the acidic environment, in which the reaction was conducted, contributes to the breaking of the siloxane bond and implicitly of the diamine into monoamines which will be converted to the corresponding Schiff bases. Analysis of the sample extracted from the reaction mixture before the addition of the copper salt confirms the breaking of the siloxane bond.

The crystallographic analysis revealed the asymmetric structural unit to be consisted from dinuclear neutral species co-crystallized with water molecules in 1:2 ratios, $[\text{Cu}_2\text{L}^1\text{L}^2\text{Cl}(\text{H}_2\text{O})]$ ($\text{L}^1 = 3\text{-FSA}$, $\text{L}^2 =$ derived azomethine), (**Figure 1b**). Two such adjacent dinuclear units are further interacting through additional $\text{Cu}_1 \cdots \text{O}_7'$ of 2.9124(1) Å and $\text{Cu}_2 \cdots \text{O}_5'$ of 2.6334(1) Å coordination with the formation of centrosymmetric tetranuclear units $[\text{Cu}_4(\text{L}^1)_2(\text{L}^2)_2\text{Cl}_2(\text{H}_2\text{O})_2]$, as shown in **Figure 1c** [7].

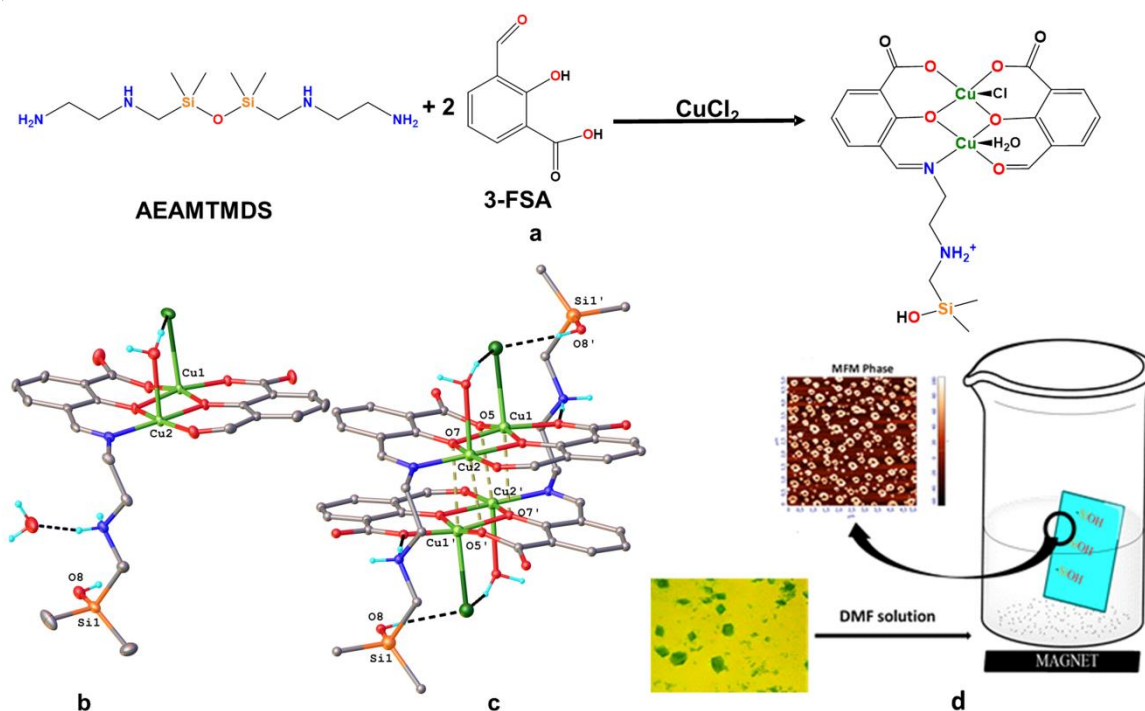


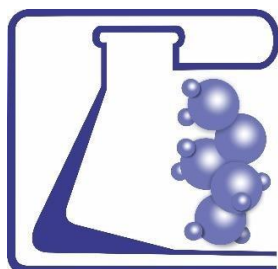
Figure 1. Pathway leading to copper complex, $[\text{Cu}_2\text{L}^1\text{L}^2\text{Cl}(\text{H}_2\text{O})]$ (a); structure of dinuclear unit (b); assembled tetranuclear unit, $[\text{Cu}_4(\text{L}^1)_2(\text{L}^2)_2\text{Cl}_2(\text{H}_2\text{O})_2]$; (c); attachment of the complex by the Si-OH group to the glass surface (d) [7].

Highly reactive free silanol arms allow the covalent attachment of the complex to suitable solid substrates, in this case glass. Their presence on the glass surface was highlighted by AFM and MFM images (**Figure 1d**). The possibility of immobilization on a solid, insoluble substrate creates the premises for a high efficient valorization of the compound in applications such as single layered sensing or heterogeneous catalysis [7].

References

- [1] M. Baral, A. Gupta, B. K. Kanungo, *AIP Conf. Proc.*, 2015, 1675, 020018-1–020018-5.
- [2] F.S. Nworie, *J. Anal. Pharm. Res.*, 2016, 3(6), 00076.
- [3] A. D. Khalaji, in *Current Trends in X-ray Crystallography*, Chapter 7: Structural Diversity on Copper(I) Schiff Base Complexes, Ed. InTech Open, 2011, p. 161-191.
- [4] J. L. Sague Doimeadios, Silver coordination compounds with a family of ditopic ligands of varying flexibility: about chains, rings, helices and polycatenanes, Doctoral Thesis, Basel, 2006.
- [5] C. Li, C. Zuo, H. Fan, M. Yu, and B. Li, *Thermochim. Acta*, 2012, 545, 75-81.
- [6] R. J. Perry, G.L. Soloveichik, M.I. Rubinstajn, M.J. O'Brien, L.N. Lewis, T.H. Lam, S. Kniajanski, D. Hancu, Patent US 9,956,520, 2018.
- [7] A.-C. Stoica, M. Damoc, V. Tiron, M. Dascalu, A. Coroaba, S. Shova, M. Cazacu, *J. Mol. Liq.* 2021, 344, 117742.

Acknowledgment: This work was supported by a grant of the Ministry of Research, Innovation and Digitization, CNCS/CCCDI – UEFISCDI, project number PN-III-P4-ID-PCE-2020-2000, within PNCDI III (Contract 207/2021, PerMONSiI).



PETRU PONI